# Parametric and numerical modelling tools to forecast hydrogeological impacts of a tunnel

**Valentina Vincenzi, Leonardo Piccinini, Alessandro Gargini and Michele Sapigni**

**Abstract:** The project of a hydro electrical diversion tunnel through a crystalline rock massif in the Alps needed a detailed hydrogeological study in order to forecast the magnitude of water inflows inside the tunnel and the possible effects on groundwater flow. The tunnel has a length of 9.5 km and is located on the right side of Toce River at Crevoladossola (Verbania province, Piedmont region, Northern Italy). In the geological framework of the Alps, the tunnel is located inside the Lower Penninic Nappes, in the footwall of the Simplon Normal Fault; the geological succession is mostly represented by Antigorio gneiss (meta-granites) and Baceno metasediments (meta-carbonates). Due to the presence of important mineralized springs used for commercial mineral water, the hydrogeological study focuses both on quantity and quality aspects, by means of: rainfall data analyses, monitoring of major springs flow rates, monitoring of hydraulic heads and pumping rates of existing wells/boreholes, hydrochemical and isotopic analyses on springs and boreholes and hydraulic tests (Lefranc and Lugeon). The resulting conceptual model evidences a dominant low permeability (aquitard behaviour) of gneissic rock masses, except for situations of intense fracturing due to tectonization, and an aquifer behaviour of metasediments, particularly when interested by dissolution. Groundwater flow systems are mainly controlled by gravity. Springs located near Toce river are characterized by higher mineralization and isotopic ratios, indicating long groundwater flow paths. Starting from all the data collected and analyzed, two parametric methods are applied: 1) Dematteis method (Dematteis et al., 2000), slightly adapted to the case study and to the available data, that allows assessing both potential inflows inside the tunnel and potential impact on springs (codified as Drawdown Hazard Index); 2) Cesano method (Cesano et al., 2000) that allows only assessing potential inflows inside the tunnel, discriminating between major and minor inflows. Contemporarily a groundwater flow model is implemented with the EPM (Equivalent Porous Medium) approach, using MODFLOW-2000; it is calibrated in steady state conditions on the available data (groundwater levels inside wells/piezometers, elevation and flow rate of springs). Dematteis method proves to be more reliable and more adequate to the site than Cesano one; it was validated on a tunnel in gneissic rock masses and it takes more into account intrinsic parameters of rock masses than morphological and geomorphological factors. Cesano method relatively overestimates tunnel inflows, taking more into account the variations of topography and overburden above the tunnel. A sensitivity analyses evidences a low sensitivity of parametric methods to parameters values, except for RQD (Rock Quality Designation) used to represent fracturation degree. The numerical model is calibrated in ante-operam conditions and a sensitivity analysis evaluates the influence of uncertainties in hydraulic conductivity (K) values of the different hydrogeological units. Hydraulic head distribution after tunnel excavation is forecasted considering three different scenarios: tunnel only draining; tunnel as a losing source of water; tunnel sealed along its aquifer sectors, using 3 different levels of K reduction. Tunnel impermeabilization results very effective, lowering the drainage rate and the impact on springs. The model defines quantitatively the tunnel inflows and the effects on springs flow at the surface in terms of flow rate decrease. Dematteis method and the numerical model are crossed to obtain a final risk of impact on springs. The study is supposed to overestimate the risk, because all the values assigned to parameters are chosen in a conservative way and numerical simulations at steady state are very conservative too (transient state in such a hydrogeological setting is supposed to last 1-3 years). Monitoring of tunnel and springs during tunnel boring will allow the feedback process.

**Keywords:** tunnel, groundwater inflow, forecasting, spring, impact.

**Valentina VINCENZI**
Geotema S.r.l., Ferrara,
via Piangipane 141 int.5
44121 Ferrara
Tel. 0532.1862693
Fax 0532.1862767,
vincenzi@geotema.it

**Leonardo PICCININI**
Dipartimento di Scienze della Terra
via G. Saragat 1
44121 Ferrara
leonardo.piccinini@unife.it

**Alessandro GARGINI**
Dipartimento di Scienze della Terra
via G. Saragat 1
44121 Ferrara
gga@unife.it

**Michele SAPIGNI**
Enel Produzione S.p.A
via Torino 16
10132 Venezia-Mestre
sapigni.michele@enel.it

Received: 7 october 2010 / Accepted: 18 november 2010
Published online: 31 december 2010



**Riassunto:** *Il progetto di costruzione di una galleria di derivazione attraverso rocce cristalline nelle Alpi occidentali ha richiesto un dettagliato studio idrogeologico finalizzato alla previsione delle venute d'acqua in galleria e dei possibili effetti sulla circolazione idrica sotterranea. Il tunnel ha una lunghezza di 9,5 km e si trova lungo il fianco destro del Fiume Toce nei pressi di Crevoladossola (Provincia di Verbania, Regione Piemonte). Dal punto di vista geologico regionale, il tracciato della galleria attraversa le Falde Pennidiche Inferiori costituite da potenti falde gneissiche (meta-graniti; Verampio, Antigorio, M. Leone) alternate a più sottili orizzonti metase-*


DOI 10.4409/Am-021-10-0017

*dimentari (principalmente meta-carbonati; Teggiolo e Baceno) in origine corrispondenti all'originaria copertura triassico-cretacica del basamento cristallino. Questa struttura a sandwich ha assunto l'attuale conformazione a duomo durante il sollevamento a letto della faglia normale del Sempione. La presenza, nei pressi del tracciato, di importanti sorgenti mineralizzate utilizzate a scopo potabile e commerciale ha imposto uno studio idrogeologico basato sia su dati quantitativi che qualitativi (misure di precipitazione, monitoraggio delle portate delle sorgenti, monitoraggio dei livelli piezometrici nei sondaggi e risultati di prove di emungimento in pozzi e sondaggi esistenti, prove idrauliche Lefranc e Lugeon nei sondaggi e monitoraggi idrochimici e isotopici sulle sorgenti e sui sondaggi).*

*Dall'analisi del modello geologico e dei dati idrochimici è stato definito il modello idrogeologico concettuale di riferimento che assegna un comportamento acquitardo alle rocce gneissiche, ad eccezione delle fasce tettonizzate e fratturate, ed un comportamento acquifero ai metacarbonati in particolare dove interessati da fenomeni di dissoluzione. Le sorgenti localizzate sul fondovalle del fiume Toce, caratterizzate da una maggiore mineralizzazione e maggiori rapporti isotopici, costituiscono il recapito di lunghi percorsi sotterranei all'interno di un sistema di flusso idrico sotterraneo essenzialmente controllato dalla gravità.*

*Sulla base del modello geologico e di tutti i dati raccolti sono state effettuate previsioni d'impatto con due metodi parametrici e un modello numerico. Il primo metodo parametrico utilizzato (Dematteis et al., 2000), leggermente modificato per adattarlo al caso in esame, ha consentito di valutare sia le potenziali venute d'acqua in galleria sia i possibili impatti sulle sorgenti (definiti come Drawdown Hazard Index); il secondo metodo parametrico (Cesano et al., 2000) ha consentito solamente la determinazione delle potenziali venute d'acqua in galleria discriminando tra maggiori e minori. Parallelamente è stato costruito un modello numerico alle differenze finite (MODFLOW-2000) dell'intero massiccio montuoso assumendo un comportamento poroso equivalente (EPM) e calibrato in condizioni stazionarie sulla base dei livelli piezometrici nei pozzi e sondaggi e sulla base della quota e portata delle sorgenti.*

*Il metodo Dematteis si è dimostrato più affidabile e adeguato al caso specifico rispetto al metodo Cesano; infatti, il primo, validato su una galleria in rocce gneissiche, assegna maggiore importanza ai parametri intrinseci degli ammassi rocciosi piuttosto che ai fattori morfologici e geomorfologici. Il metodo Cesano sovrastima, relativamente agli altri metodi, le potenziali venute d'acqua in galleria assegnando più importanza alle variazioni topografiche ed allo spessore della copertura rocciosa della galleria. È stata effettuata un'analisi di sensitività sia per i metodi parametrici che per il modello numerico; i primi hanno evidenziato variabilità legata essenzialmente al valore di RQD (Rock Quality Designation, utilizzato come rappresentativo delle condizioni di fratturazione), il modello numerico è risultato influenzato dall'incertezza sui valori della conducibilità idraulica degli ammassi rocciosi. Gli effetti dello scavo sulla superficie piezometrica, preventivamente simulata in condizioni ante-operam, sono stati simulati utilizzando, nel modello numerico, tre possibili condizioni: galleria drenante, galleria disperdente ed infine galleria impermeabilizzata in corrispondenza dei settori acquiferi (con assegnazione di crescenti livelli di riduzione della permeabilità). Il trattamento dei settori acquiferi è risultato particolarmente efficace riducendo il drenaggio e gli impatti sulle sorgenti; il modello è in grado di definire quantitativamente le venute d'acqua in galleria e gli effetti sulle sorgenti in termini di riduzione della portata. L'assegnazione del livello di rischio finale per ciascuna sorgente è stato definito incrociando i risultati del modello numerico con quelli del metodo Dematteis; tali livelli di rischio sono, tuttavia, da considerarsi sovrastimati in quanto i valori assegnati a ciascun parametro sono stati scelti conservativamente ed altrettanto conservativamente si possono considerare le condizioni stazionarie generate dal modello numerico dato che, in questo tipo di ammassi rocciosi, è probabile che le condizioni transitorie si protraggano da 1 a 3 anni. Il monitoraggio delle venute d'acqua in galleria durante il futuro scavo e il proseguimento dei monitoraggi sulle sorgenti consentirà una verifica dei modelli e fornirà importanti informazioni sperimentali.*

## Introduction

In mountain regions, tunnel excavation can be the most threatening activity on groundwater and this has not ever been considered of great importance in the past, as demonstrated by various Italian case studies: the huge groundwater level drawdown and springs dewatering as a consequence of the Gran Sasso highway tunnel boring (Petitta & Tallini, 2002), but also in recent times the impact on streams and springs due to the tunnels of the Bologna-Florence high-speed railway line (Gargini et al., 2006, 2008). As a consequence, in the last years people and authorities have become more and more sensitive to the problem and the scientific attention has been drawn on the possibility to forecast the effects of tunnels and underground excavations concerning groundwater inflows and water table drawdown and to evaluate the risk for springs located in the hydrogeological basin crossed by the underground opening.

The forecasting of the impacts of a draining tunnel on groundwater flow systems is one of the most challenging tasks in engineering geology. Tunnel drainage can produce severe effects on hydrogeological systems, either at transient or at steady state conditions, such as springs drying out, hydraulic head drawdown and wells yield shortage, streams base flow depletion. The resulting environmental, socio-sanitary and economic damages, if forecasted at the early stage of the project, should address risk mitigation measures (alternative tunnel pathways, tunnel sealing, even the project abandonment) in the framework of a technically correct cost-benefit analysis.

In hard rock aquifers it's extremely difficult to forecast either major inflows occurrence along the tunnel or the associated effects on surface waters and groundwater, due to the highly heterogeneous distribution of hydraulic conductivity (K) and the consequent strong dependence of major inflows on the interception of localized geological features (i.e. fractured zones, faults, karst conduits). Their geometry and locations can be achieved by means of a good 3D geological model (geological mapping, aerial-photos interpretation and geophysical surveys) with an approximation of some tens or hundreds of meters and, only in a few cases, it's possible to determine their hydraulic parameters by means of permeability tests performed in deep boreholes.

Two different evaluation tools are addressed in order to overcome these uncertainties and to get a good forecast: parametric methods and mathematical models.

Parametric studies, also known as matrix methods, identify relevant physical quantities (such as RQD, permeability, overburden, faults intersecting the tunnel) and rank them and their interactions by assigning ratings and multipliers to gain final probability indexes of impact on each spring. Parametric methods for an impact assessment evaluation can be matrix-based or rating & weight based. In the first case a contingency matrix is developed, crossing together relevant parameters: the classical example is the Leopold matrix for

EIA (Environmental Impact Assessment, Leopold, 1971). In the second case a parameterization system of ratings and multiplier weights is applied to variables considered as relevant, in order to obtain final quantification indexes: typical examples are given by DRASTIC (Aller et al., 1985) and SINTACS R5 (Civita & De Maio, 2000) methods, made to assess aquifers intrinsic vulnerability.

On the other hand, mathematical groundwater flow modelling simulates the actual process causing the impact with a physically based approach. Adopted simulation codes vary from simple analytical formulas, assuming a Darcyan groundwater flow, simple and stationary boundary conditions and homogenous or simple K distribution (Zhang & Franklin, 1963; Goodman, 1965; Barton, 1974; Federico, 1984; Lei , 1999, 2000; El Tani, 1999), to complex numerical codes, more flexible and adjustable to real world conditions but much more exigent in terms of scientific expertise, financial resources and input data.

In the here presented case study the occurrence of important mineralized springs used for commercial mineral water asked for a solid risk analysis. The potential impacts on springs due to a draining tunnel were so evaluated applying the two different methods: the parametric probabilistic and the numerical deterministic. Both methods started from a detailed hydrogeological study necessary to set up the conceptual model and the final drawdown risk of each spring were obtained from the convergence of the two methods. This paper presents the main results, together with the effectiveness of the two approaches in performing such risk analysis.

## Geological setting

The diversion tunnel layout crosses the deepest part of the Penninic Units traditionally assigned to the ancient northern margin overthrusted by the oceanic and the southern austroalpine margin during the continental collision of the alpine orogenesis. The present-day deep topographic erosion allows a glimpse onto the structure of the Lepontine nappes, tectonic units formed by flat recumbent folds consisting of orthogneissic cores with discontinuous micaschistic and paragneissic outer zones overlaying mesozoic metasediments (Schmidt & Preiswerk, 1905; Castiglioni, 1958; Milnes et al., 1981; Steck, 2008) (Fig.1). The latter are composed of calcschists, dolomitic and calcitic marbles, quartzites and discontinuous gypsum and anhydritic horizons. This petrographic and rheologic sandwich is the result of many deformative phases, the most important of which sliced and thrusted the former continental, mainly granitic, crust onto the sedimentary cover with displacements of tens of kilometres (Maxelon & Mancktelow, 2005). The amphibolitic metamorphic conditions achieved during the main deformation phase allowed the mineralogical transformations that gave place to the pervasive axial plane foliation forming the present-day schistosity and most prominent weakness planes of the rock mass. Successive slightly or non metamorphic folding events gave the nappe pile its present dominant structure visible along the Antigorio valley (Fig. 2) with a flat laying attitude in its central part, around the so called Verampio window, passing to a steep southward inclination near Crevoladossola (Mancktelow, 1985; Grasemann & Manktelow, 1993). The N-S cross

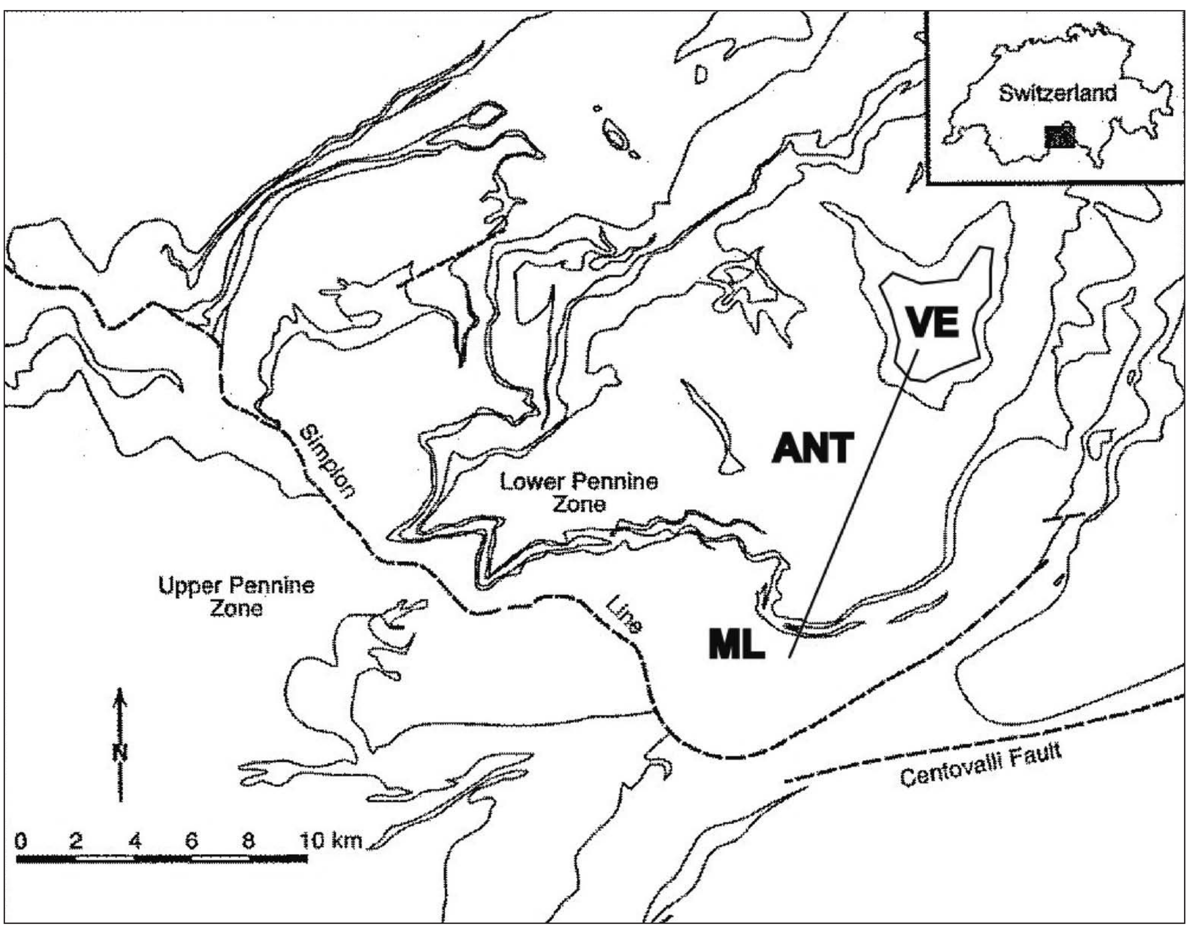


**Fig. 1:** *Geological sketch of the area between the Verampio window (VE) and the Simplon Fault (modified from Grasemann & Mancktelow, 1993). ANT: Antigorio gneiss; ML: Monte Leone gneiss. The line represents the trace of the cross section of figures.2 and 3.*

 DOI 10.4409/Am-021-10-0017

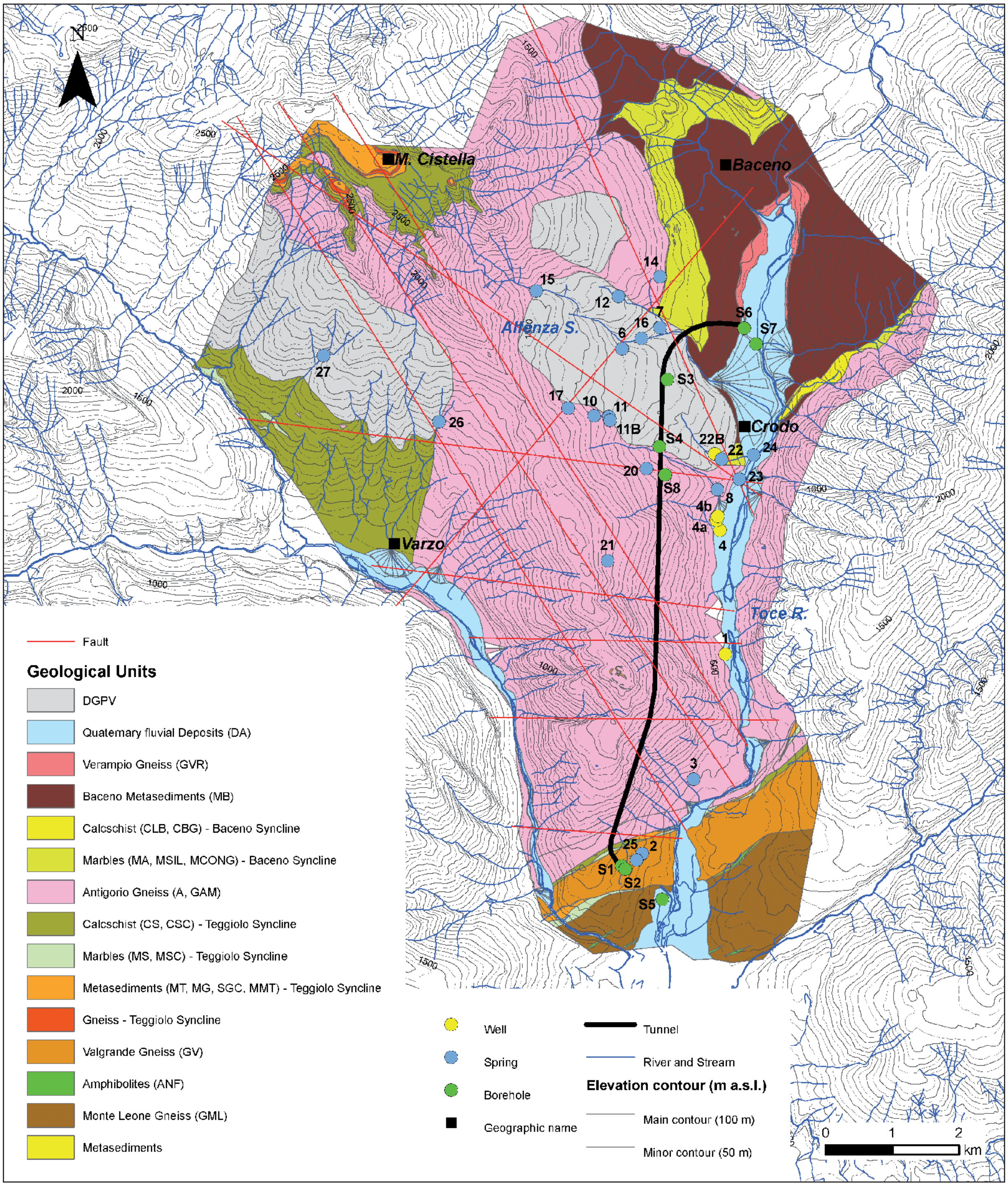


**Fig. 2:** *Geological map of the study area, with groundwater monitoring points.*

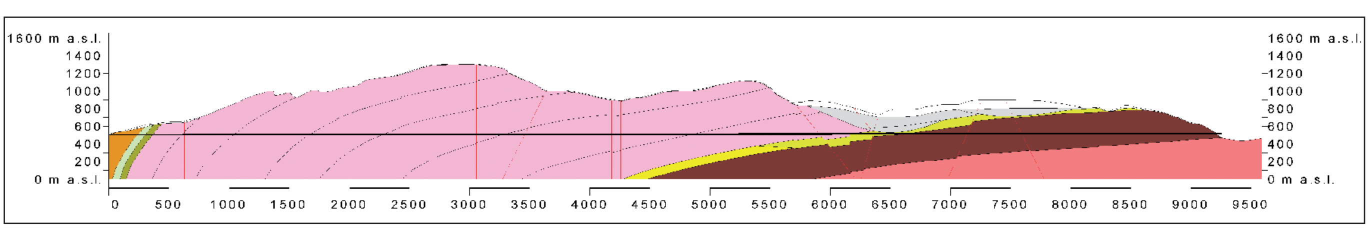


**Fig. 3:** *Geological section along the tunnel; colors according to geological legend in Fig. 2.*

section (Fig. 3) shows the geologic and hydrogeologic structure of the mountain ridge and corresponds to the trace of the diversion tunnel, presented on the geological map of Figure 2. The main feature is represented by the thick late Variscan (ca. 340 My) Antigorio unit, composed of a monotonous leucocratic orthogneiss that only rarely shows any structural or petrographic diversity (Bigioggero et al., 1977). To the north it overlays the deepest alpine unit corresponding to the as well late Variscan Verampio granitic gneiss and its host rock represented by the garnet-rich Baceno micaschists. Interlayered between this two big tectonic units is located the most important permeable unit (Baceno metasediments), which stratigraphy has been well defined after the drilling of three deep boreholes. It has an average thickness around 70 meters and is composed by a lower gypsum-anhydrite layer, at least two cohesionless sugary carbonate horizons, dolomitic marbles and calcschists. To the south the geological structure is characterised by a late non-metamorphic kilometre-scale fold linked to the exhumation of the nappe pile along the extensional Simplon Fault (Campani et al., 2010). Near the southern portal the tunnel trace crosses the second metasedimentary unit (Teggiolo) around 70 meters thick and with a composition very similar to the Baceno metasediments. The tunnel trace ends in the third gneissic continental unit (Valgrande gneiss) mainly composed of fine grained quartz-micaschists and grey biotitic gneiss.

Detailed geological mapping, boreholes and geophysics allowed both to reconstruct a reliable 3D model and to recognise a huge deep seated landslide (Deep Seated Gravitational Deformation, DSGD) in the northern part of the section that might be genetically linked to the underlying weak metasedimentary horizon. The whole triangular shaped ridge is cross-cut by many brittle faults arranged in two main sets NW-SE and E-W oriented; they are the product of the brittle last exhumation phase of the Lepontine dome along the Simplon Fault (Bistacchi & Massironi, 2000; Grosjean et al., 2004; Zwingmann & Mancktelow, 2004).

## Materials and methods

### *Hydrogeological characterization*

The occurrence of important mineralized springs used for commercial mineral water asked for an hydrogeological study focused both on quantity and on quality of groundwater; the study has been developed by applying different tools.

A rainfall data analysis, based on 8 meteorological stations, has been performed in order to estimate the recharge rate to the aquifers. The water surplus on the modelled area has been calculated by means of Thornthwaite & Mather (1957) soil water balance.

A census of the main water points was available, together with one year of hydrogeological monitoring in ante-operam conditions on 21 major springs and 5 wells in the area. Furthermore, 8 boreholes bored for the project were available for hydrogeological monitoring (Table 1). The available data (collected by CESI S.p.A) were: flow rates at springs and groundwater levels at wells and boreholes, measured on a monthly basis. The DVI (Discharge Variability Index) has been calculated for all the springs as (Qmax-Qmin)/Qav, where Qmax is the maximum flow rate, Qmin the minimum flow rate and

**Tab. 1a:** *Main hydrogeological and hydrochemical data of springs.*

| ID | Name | Type | Altitude (m a.s.l.) | Average flow rate (l/s) | IVP | α ($d^{-1}$) | Hydrochemical facies |
|---|---|---|---|---|---|---|---|
| 2 | Bisogno | Spring | 890 | 0.02 | | | |
| 3 | Oira | Spring | 420 | 11.17 | 0.83 | 1.29E-02 | Ca-$HCO_3$-$SO_4$ |
| 6 | Viceno | Spring | 850 | 3.07 | 0.31 | 6.50E-04 | Ca-Mg-$SO_4$-$HCO_3$ |
| 7 | La Valle | Spring | 850 | 5.38 | 0.28 | 3.00E-04 | Ca-$HCO_3$ |
| 8 | Vegno | Spring | 510 | 1.55 | 2.19 | 2.33E-02 | Ca-Mg-$SO_4$-$HCO_3$ |
| 10 | Flecchio alta | Spring | 1170 | 0.23 | 1.22 | 1.11E-02 | Ca-$HCO_3$ |
| 11 | Flecchio | Spring | 1100 | 14.22 | 0.73 | 1.13E-02 | Ca-$HCO_3$ |
| 11b | Flecchio Isolata | Spring | 1090 | 3.23 | 1.47 | | Ca-$HCO_3$ |
| 12 | Longio | Spring | 1140 | 16.04 | 0.49 | | Ca-$HCO_3$ |
| 14 | Trona | Spring | 1050 | 1.37 | 0.88 | 3.10E-03 | Ca-$HCO_3$ |
| 15 | Alfenza Nord | Spring | 1420 | 12.46 | 1.05 | | Ca-$HCO_3$ |
| 16 | Alfenza sud | Spring | 874 | 2.31 | 0.91 | 2.95E-03 | Ca-$HCO_3$ |
| 17 | Cavoraga-Faiò | Spring | 1300 | 0.08 | 1.38 | 9.40E-03 | Ca-$HCO_3$-$SO_4$ |
| 20 | Ronconi | Spring | 890 | 0.56 | 0.96 | 1.19E-02 | Ca-$HCO_3$ |
| 21 | Cheggio | Spring | 1390 | 0.06 | 1.19 | 1.91E-02 | Ca-$HCO_3$-$SO_4$ |
| 22 | Cesa Inferiore | Spring | 545 | 0.20 | 0.74 | 2.10E-03 | Ca-$HCO_3$ |
| 23 | Valle Oro | Spring | 457 | 19.97 | 0.11 | 6.60E-03 | Ca-$SO_4$ |
| 24 | Lisiel | Spring | 470 | 34.96 | 0.06 | 4.00E-04 | Ca-$SO_4$-$HCO_3$ |
| 25 | La Conca | Spring | 470 | 0.18 | 1.00 | 4.55E-03 | Ca-$HCO_3$ |
| 26 | La Rocca | Spring | 1100 | 15.00 | | | |
| 27 | Calantagine | Spring | 1420 | 35.00 | | | |


DOI 10.4409/Am-021-10-0017

**Table 1b**: *Main hydrogeological and hydrochemical data of wells and boreholes.*

| ID | Name | Type | Altitude (m a.s.l.) | Depth (m) |
|---|---|---|---|---|
| 1 | Sarizzo | Well | 386 | 30 |
| 4 | Molinetto1 | Well | 424 | 101 |
| 4a | Molinetto2 | Well | 424 | 54 |
| 4b | Molinetto3 | Well | 424 | 71 |
| 22b | Cesa | Well | 573 | 33 |
| S1 | | Borehole | 508 | 11.3 |
| S2 | | Borehole | 529 | 35.5 |
| S3 | | Borehole | 883 | 376 |
| S4 | | Borehole | 792 | 304 |
| S5 | | Borehole | 308 | 30 |
| S6 | | Borehole | 518 | 15 |
| S7 | | Borehole | 517 | 15 |
| S8 | | Borehole | 811 | 412 |

Qav the average flow rate, relatively to the monitored year; the α coefficient (recession coefficient according to Maillet, 1905) has been also calculated for each spring, deriving it from the recession curves of the available data.

Together with the flow and piezometric measurements, in-situ physico-chemical parameters have been measured by means of a multi-parameter probe (temperature, specific electrical conductivity, pH, dissolved oxygen and dissolved carbon dioxide).

In the laboratory, ionic concentrations of fluoride, chloride, sulphate, nitrate, sodium, potassium, magnesium and calcium together with alkalinity, dissolved silica and fixed residue, have been measured on groundwater samples collected at the monitoring network on a monthly basis; concentrations of Iron (total), Strontium and Lithium have been measured twice a year at 5 monitoring points (11, 12, 22b, 23 and 24; Table 1); isotopic ratios of $\delta^2H$, $\delta^{18}O$ (standard VSMOW as in Craig, 1961) and $\delta^{13}C$ (standard PDB as in Urey et al., 1951) have been measured on a monthly basis at the 4 most important monitoring points (11, 22, 23 and 24, chosen for their high discharge rates as well as for their drinkable and commercial use).

Main data concerning monitoring and classification of water points (springs, boreholes and wells), coming both from the census and from data interpretation, are summarized in Table 1.

Geological units have been classified with respect to the permeability type (porous or fractured media) and to the expected K values, which have been derived from the combined use of geological and geomorphological information available in literature, performed permeability tests (Lefranc and Lugeon tests) inside 8 boreholes in the area and other tests performed 30 years ago for the planning of Piedilago-Agaro plant, located 7 km to the north but in the same geological units (Martinotti per ENEL Produzione, 1993).

Springs have been classified according to Civita (1973, 2005) and the conjunctive analysis of all the data allowed to set up the hydrogeological conceptual model.

## Parametric methods

A parametric method applied to tunnel impacts forecasting is basically a risk assessment where the risk of a damage occurring to groundwater as a result of the tunnel drainage is evaluated. Analyzing the general formula (Einstein, 1988) in terms of tunnel impacts:

$$\mathbf{R = H * P * Va * V} \qquad (1)$$

**R** is the risk, e.g. the occurrence probability of an impact against groundwater flow systems;
**H** is the hazard, e.g. the magnitudo of the impact process, e.g. a major inflow at the tunnel face;
**P** is the hazard Probability that a major inflow could occur along the tunnel;
**Va** is the receptors Value, that means the environmental, hydrologic and socio/economic importance of springs, streams and wells (surface emergence of groundwater flow systems) potentially subject to impact;
**V** is the vulnerability, intended as the expected damage in relationship to major inflow occurrence due to the hydrogeological connection between tunnel and receptors.

Two methods, validated by case histories in metamorphic rocks similar to those of our study, have been chosen: DHI or Dematteis method (Dematteis et al., 2001) and Cesano method (Cesano et al., 2000). These methods consider a multiple set of parameters increasing the confidence in the probabilistic evaluation respect to single-parameters method (Thapa et al., 2005). They were partially modified for the intended application, in order to overcome either the lacking of data measured at the tunnel drilling face (the study was done in ante-operam condition), available in the original application of the methods, or some intrinsic limitations of the method in the final DHI output.

Whole tunnel trace (about 9000 m) has been divided in 50.1 m length sectors, with a total of 183 sectors (progressively numbered from northern to southern portal). The average elevation of each sector was assigned at the middle, depending on the linear gradient (9.05 ‰) between two main portals elevation, from 513.3 m (north) to 505 m a.s.l. (south).

A total of 21 springs and 5 wells were considered as potential impact receptors for DHI evaluation, according the hydrogeological conceptual model. Hydrogeological structure, groundwater flow circuits depth and springs hydrochemistry contributed to define the degree of hydrogeological connection between the receptors and the tunnel sectors.

## Application of DHI method

DHI method is a typical rating and weight parametric method for the evaluation of Risk, expressed by an index called "DHI" (Drawdown Hazard Index) ranking the probability of spring flow depletion in relationship to inflow probability occurrence and spring vulnerability. DHI method is a fully-coupled-model (Jiao & Hudson, 1995) and takes into account the physical relationships of different variables. The method is applied through two steps: firstly, variables affecting the probability of PI (Potential Inflow) generation inside tunnel sectors are rated and weighted; secondly, the obtained PI value is further weighted, in relationship to local vulnerability, in order to obtain the final DHI value.

The original formulas from Dematteis et al. (2001) are:

$$\mathbf{PI(n)= (0.41*FF(n)+0.22*RMP(n) +0.20*PZ(n)+0.17*OV(n))} \qquad (2)$$

$$\mathbf{DHI(spring)=(PI)\ (average)*(IF+1)*(ST+1)*(DT+1)} \qquad (3)$$

where **FF** = rock-mass fracture frequency; **RMP** = rock mass hydraulic conductivity; **PZ** = thickness of the Plastic Zone around the bored tunnel; **OV** = tunnel Overburden, including Quaternary deposits; **IF** = occurrence of hydrogeologic connection between spring and tunnel; **ST** = spring type, related to the depth of groundwater flow system discharging at the spring; **DT** = geometric distance between the tunnel sector and the spring.

DHI is ranked in four piezometric drawdown risk classes with a relative probabilistic output, as shown in Table 2.

**Tab. 2:** *DHI classes according Dematteis method.*

| DHI | DHI classes |
|---|---|
| < 0.2 | Absence of (or minimal) Drawdown |
| 0.2 ÷ 0.6 | Moderate Drawdown |
| 0.6 ÷ 0.7 | From moderate to severe Drawdown |
| > 0.7 | Spring drying-up |

With respect to the original formulation (see Dematteis et al., 2001) the following changes have been introduced.

FF variable: the RQD index (Rock Quality Designation) (Deere et al., 1969; Deere & Deere, 1989), derived from boreholes S1-S2-S3-S4 and S8, was considered representative of FF, because geomechanical surveys at the drilling face were not available. An average arithmetic mean of RQD values has been calculated for each geological unit; the obtained results have been integrated with data coming from the geomechanical surveys performed on rock mass outcrops (Astolfi & Sapigni, 1999). As a further refinement, fractures occurrence at megascale was derived from photo-aerial lineament traces intersecting the tunnel trace and it has been taken into account as follows: if a lineament occurs inside a 250 m radius cylindrical buffer zone coaxial with the tunnel, FF rating for tunnel sectors involved along ±100 m linear distance from the lineament is lowered down by one or two rating classes, respectively if 1 or more than 1 lineaments are involved.

K: permeability values were assigned to the different rock masses taking into account both Lugeon tests results and reference data, available in literature, corresponding to metamorphites in analogous geological framework (Loew, 2002). Moreover, K values have been increased of 1 order of magnitude for the tunnel sectors crossed by a fault or main fracture (with a ±50 m buffer zone) derived by the longitudinal geologic profile and for sectors crossing the contact between Antigorio Gneiss and Teggiolo Syncline, due to its important and recognized aquifer behaviour.

OV: it was derived from tunnel longitudinal section, measured at the midpoint of the corresponding sector and it ranges between 28 and 801 m.

PZ: according to a conservative approach, PZ value was always considered equal to three times the maximum calculated EDZ (Excavation Disturbed Zone) reaching the conservative value of 14.7 m.

IF: a 100 m and 50 m buffer zone has been defined for each side of, respectively, primary or secondary structural lineaments (obtained by field geological survey or aerial photos interpretation). If a spring is located inside the buffer zone and, at the same time, the lineament crosses the tunnel, the spring IF value is 1 (otherwise it is 0). Springs discharging out from quaternary deposits always received a 0 rating, because these deposits are never involved by tunnel boring.

ST: three main groundwater flow systems have been identified according to springs classification: shallow, deep and mixed, receiving respectively a 0, 1 and 0.5 rating.

DT: Euclidean distance (e.g. minimum geometrical distance) between the midpoint of each tunnel sector and the receptors has been calculated independently of the relative elevation of the receptor respect to the tunnel. DT range is between 8907 and 244 m.

## Application of Cesano method

Cesano method actually is not a codified parametric method but a study showing the results of a multi-regression analysis between tunnel potential inflows and affecting variables in an analogous hydrogeological framework (gneissic fractured aquifer below a variable thickness of Quaternary cover) for a 80 km long tunnel in southern Sweden (Cesano et al., 2000). It was chosen as a further evaluation tool, proposing a different set of PI factors, in order to better verify the results. Cesano method does not evaluate DHI but only PI, discriminating major inflows from diffuse dripping. Four major inflows factors, among many others, are recognized and listed here in order of importance: TSW = tunnel proximity to a main surface water body (i.e. streams, lake, reservoir); BM = bedrock morphology underlying Quaternary cover; T = topography; BFF = bedrock aquifer fracture density. Four diffuse dripping factors, among many others, are recognized and listed here in order of importance: BM = bedrock morphology underlying Quaternary cover; QC = thickness and lithology of Quaternary cover; QA = area of Quaternary outcrops above the tunnel; PV = peaks and valleys occurrence of BM.

The main change introduced to Cesano method was to transform the multi-factorial correlation analysis of the original method into a rating and weighting parametric method, by summing the correlation coefficients and normalizing the result to 1. In such a way a weighted linear combinations of rates allowed a coherent comparison with Dematteis method. In Table 3 the weights derived for the Cesano method are presented.

**Tab. 3:** *a) Weights for major inflows factors; b) Weights for diffuse dripping factors (Cesano method).*

| a) Major inflow factor | Weight | b) Diffuse dripping factor | Weight |
|---|---|---|---|
| TSW | *0.32* | BM | *0.30* |
| BM | *0.29* | QC | *0.29* |
| T | *0.28* | QA | *0.26* |
| BFF | *0.11* | PV | *0.11* |

Relevant variables were parameterized as follows:

TSW: it is expressed by the Euclidean distance between the midpoint of each tunnel sector and the nearest main stream bed located above the tunnel. TSW values range between 9930 and 22 m; whole range was divided in 5 classes of equal amplitude.

BM and T: this two variables have been derived from Digital Elevation Model compared with tunnel longitudinal geological section, considering 200 m interval tunnel sectors in order to better represent the top of the bedrock and topographic surface elevation changes. Maximum rating (1) is applied to bedrock troughs (areas of potential concentrated recharge), minimum rating (0) to mounds; a 0.5 rating was assigned for intermediate BM values. T value range between 505 and 1299 m a.s.l.

BFF: primary and secondary megascale tectonic lineaments have been taken into account as for FF Dematteis variable. The total num-

 DOI 10.4409/Am-021-10-0017

ber of lineaments crossing the tunnel (divided in 100 m long tunnel sectors) has been calculated: ratings of 1, 0.7, 0.35 and 0 were assigned to the tunnel if the number of lineaments is, respectively, ≥ 3, 2, 1, 0.

QC: it was derived from tunnel longitudinal geological section. Maximum thickness value is 260 m, corresponding to the DSGD mass. Whole QC range has been rated according 5 different classes of equal amplitude.

QA: the outcropping areal extension (m$^2$) of QC inside a 100 m long search cylindrical volume coaxial with the tunnel and with 1000 m radius has been calculated, as derived from geomorphological map and DEM. Values range from a maximum of 99800 m$^2$ (tunnel sector completely covered by Quaternary deposits; maximum rating of 1) to a minimum of 0 m$^2$ (0 rating).

PV: peaks and valleys occurrence in the bedrock have been identified from tunnel longitudinal geological section, according to a discretization of 100 m long tunnel sectors. A rate of 0 and 1 was assigned, respectively, to peaks and valleys; a rate of 0.5 was assigned to all the other sectors.

## Numerical model

Analytical codes, generally useful for limited tunnel sector and time-scale frames (Loew, 2002), were excluded because too much simplistic for the complex hydrogeologic setting. A three-dimensional groundwater flow model has been developed by means of the MODFLOW-2000 code (McDonald & Harbaugh, 1988; Harbaugh et al., 2000), that solves the flow equation in saturated media according to the finite difference method.

Assuming that, along the 9.2 km long diversion tunnel, groundwater flow system at the whole mountain ridge scale follows the Darcy's law, the Equivalent Porous Medium (EPM) approach has been used. It consists in considering the rock matrix together with the fractures and assigning them bulk hydrodinamic properties, over a rock volume sufficiently wide to be considered statistically representative (Representative Elementary Volume - REV; Long et al., 1982; Kanit et al., 2003). Inside the REV it is assumed that fracture distribution is casual and uniform and that fracture width does not allow turbulence flow. Geometric and hydrodynamic properties of distinct fractures are not requested, small computational efforts are necessary and good results can be obtained working on wide modelling areas (Mun & Ucrhin, 2004).

A rectangular shaped model domain of 12000 x 17000 m has been set up, oriented parallel to Gauss Boaga coordinate system and extending from Torrente Diveria at north to Crevoladossola at south (Fig. 2). On the horizontal plane it is subdivided into cells of 100 x 100 m, except for the zone including the tunnel and the main springs in which a grid refinement leads to 25 x 25 m cells (Fig. 4). A great effort has been taken to get a good vertical discretization and 20 variable thickness layers have been used; layer 11 has been used to represent the tunnel plane and has a thickness that includes the plastic zone. The domain extends vertically from the topographic surface, derived from DEM, to an almost horizontal plane with elevation of 510 m a.s.l., with a very gentle gradient parallel to the tunnel slope. The total thickness of the model varies between 350 and 3000 meters. A section of the domain parallel to the tunnel trace is shown in Figure 5.

Hydraulic conductivity (K) is always assigned as an isotropic

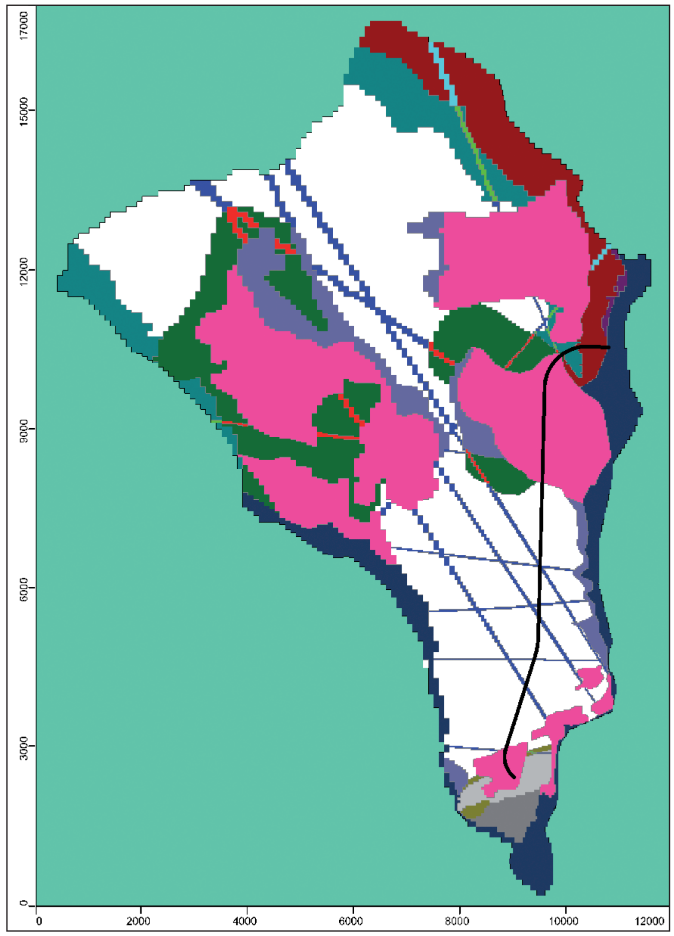


**Fig. 4:** *Flow domain and K zones at layer 1 of the MODFLOW model. Colors corresponding to K zones according to table 3; the inactive cells are represented with the green color; coordinate axis in meters; tunnel trace in black.*

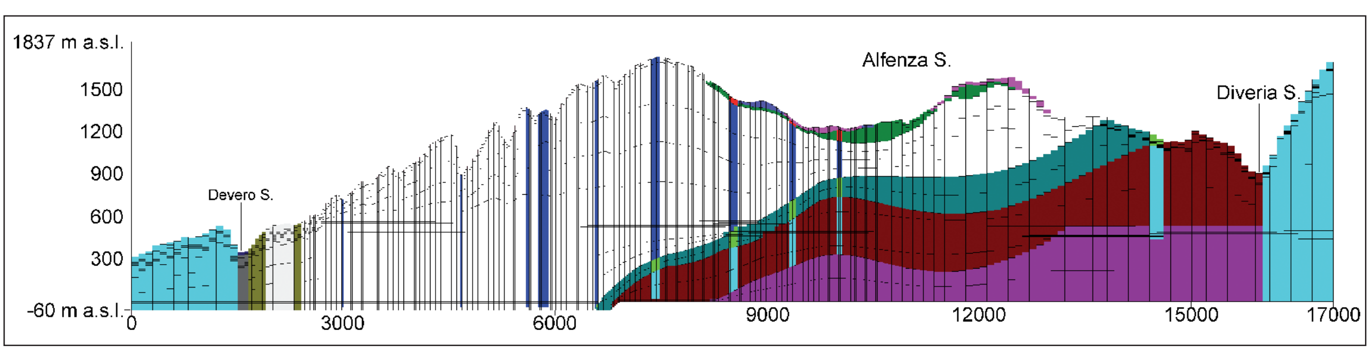


**Fig. 5:** *Section of the model domain along the tunnel trace (N-S direction), column 85: vertical discretization in 20 layers and assigned K zones (according to Table 3); vertical exaggeration of 2:1 is used.*

**Tab. 4:** *Hydraulic conductivity assigned to different K zones (in m/s).*

| Zone | Color | Hydrogeological Unit | Kx | Ky | Kz |
|---|---|---|---|---|---|
| 1 | | Antigorio gneiss | 1.00E-07 | 1.00E-07 | 1.00E-07 |
| 2 | | Quaternary fluvial deposits | 5.00E-05 | 5.00E-05 | 5.00E-05 |
| 3 | | DGPV | 7.00E-07 | 7.00E-07 | 1.00E-07 |
| 4 | | Metasediments (Baceno syncline) | 5.00E-06 | 5.00E-06 | 5.00E-06 |
| 5 | | Baceno micaschists | 1.00E-07 | 1.00E-07 | 1.00E-07 |
| 6 | | Verampio gneiss | 1.00E-08 | 1.00E-08 | 1.00E-08 |
| 7 | | Metasediments (Teggiolo syncline) | 5.00E-06 | 5.00E-06 | 5.00E-06 |
| 8 | | Valgrande gneiss | 1.00E-07 | 1.00E-07 | 1.00E-07 |
| 9 | | Monte Leone gneiss | 1.00E-07 | 1.00E-07 | 1.00E-07 |
| 10 | | Fault in Antigorio gneiss | 7.00E-06 | 7.00E-06 | 7.00E-06 |
| 11 | | Fault in Metasediments (Baceno syncline) | 1.00E-05 | 1.00E-05 | 1.00E-05 |
| 12 | | Fault in Baceno micaschists | 5.00E-07 | 5.00E-07 | 5.00E-07 |
| 13 | | Fault in DGPV | 1.00E-06 | 1.00E-06 | 1.00E-06 |
| 14 | | Quaternary glacial deposits | 5.00E-06 | 5.00E-06 | 1.00E-06 |
| 15 | | Slope debris | 5.00E-04 | 5.00E-04 | 5.00E-04 |

**Tab. 5:** *Calibration data of the ante-operam simulation.*

| Spring name (ID) | Drain conductance | Observed values | | Calculated values | | Calculated - observed | Discrepancy |
|---|---|---|---|---|---|---|---|
| | $m^2/d$ | l/s | $m^3/d$ | l/s | $m^3/d$ | $m^3/d$ | % |
| **Lisiel (24)** | 139.95 | 34.96 | 3020.5 | 34.96 | 3020.2 | -0.34 | -0.01 |
| **Valle Oro (23)** | 55.45 | 19.97 | 1725.4 | 19.97 | 1725.7 | 0.29 | 0.02 |
| **Vegno (8)** | 7.65 | 1.55 | 133.9 | 1.5 | 130.0 | -3.96 | -2.96 |
| **Cesa (22)** | 1.11 | 0.2 | 17.3 | 0.2 | 17.2 | -0.03 | -0.19 |

property, except for the normal faults/fracture zones, where an anisotropy factor of 10 resulted necessary along x and z axis during the calibration process. In Table 4 the final K values, obtained after calibration, assigned to the 15 K zones are summarized: every geological unit is represented by two K values, the first one for the normally fractured rock mass, the second one for the rock mass affected by a fault/lineament. The K zones distribution can be observed in Figure 4 and Figure 5.

Recharge to aquifer is simulated by a 2nd type boundary condition (b.c.) applied to every cell of 1st saturated layer; the low sensitivity of the model to the recharge allowed to use a uniform value of 270 mm/yr. The regional gradient is represented by a 1st type b.c. on the northern side of the domain, with a maximum head value below the mountain ridge (1800 m a.s.l.), decreasing to 1045 m a.s.l. eastward and to 1250 m a.s.l. westward. The rivers bordering the model on the western and eastern side, and representing the discharge point of regional groundwater flow system, are represented with the same b.c.: head values have been assigned equals to riverbed elevations derived from the DEM. On the eastern side head varies from 1045 to 520 m a.s.l. along Devero River and from 520 to 300 m a.s.l. along Toce River; on the western side it varies from 1250 to 530 m a.s.l. along Cairasca River and from 530 to 300 m a.s.l. along Diveria River. Cells outside the boundary conditions are switched off, so that the final shape of the domain is irregular. The 4 main springs have been represented by means of the Drain Package (3rd type b.c.), assigning to the cell a drain elevation equal to ground level at the spring. Conductance values, calibrated on the real flow rate at the springs, are: 139.95 $m^2/d$ for Lisiel spring, 55.45 $m^2/d$ for Valle Oro spring, 1.11 $m^2/d$ for Cesa spring and 7.65 $m^2/d$ for Vegno spring.

The calibration process has been performed at steady state conditions on a simulation representing the present situation and solved by means of the Link-algebraic MultiGrid solver package (Mehl & Hill, 2001). The trial & error process (Zheng & Bennevy, 1995) has mainly involved the K values and the uncertain b.c., i.e. the constant head at the northern boundary. All the 17 piezometric control points have been used, for which at least one piezometric measure was available; in Table 5 these data are presented. Flow rates of springs have been used to calibrate conductance values.

The forecasting simulations have been performed according to two different behaviors of the tunnel: in the first one, representative of the drilling phase, the tunnel is assumed completely draining, while in the second, representative of the post-operam conditions, the tunnel is supposed to be dispersant.

The draining tunnel is simulated by means of the Drain Package, that removes groundwater from the cells in which it is applied as a function of heads differences (between the aquifer and the tunnel

 DOI 10.4409/Am-021-10-0017

elevation) and of the conductance parameter around the tunnel. The drain elevation is equal to the tunnel elevation, while the Conductance (C) values (parameter that represent the resistance opposed to flow by the rock mass all around the tunnel; Zaadnoordijk, 2009), were calculated as:

$$\mathbf{C = (KPZ \times 2\pi R) / h} \tag{4}$$

where **KPZ** is the hydraulic conductivity of the Plastic Zone, **R** is the tunnel radius and **h** is the plastic zone thickness.

So, different C values have been assigned to the tunnel reaches crossing different K zones of the rock mass. A sensitivity analysis tested 3 different values of KPZ, assuming an increase of 5, 10 and 100 times the original rock mass K.

The simulation with the dispersant tunnel takes into account the inside flow rate of 18 $m^3/s$ and calculates the water exchange with the rock mass. The dispersant tunnel is represented by the Streamflow-Routing Package STR1 (Prudic, 1989), a 3rd type b.c. usually applied to simulate river-groundwater interactions, according which the stream flow rate is propagated starting from the value of the most upstream cell (starting point) and calculated for every cell downstream as the previous flow rate plus or minus the stream flow rate gained from or lost to the aquifer. The in/out flow is calculated multiplying the head difference between the stream and the aquifer times the riverbed conductance. The water level inside the tunnel is 4 meters above the tunnel bottom, while the conductance is calculated as for the draining tunnel simulation.

Finally, other simulations have been set up in order to evaluate the effects of concrete linings on the most critical sectors of the tunnel, taking into account three different K values for the plastic zone of the lining sectors: KPZ equal to the K of the drilled rock mass (A), KPZ = 0.1*K of the drilled rock mass (B), KPZ = 1E-07 m/s (C). In the sectors without linings the KPZ is 10 times the K of the surrounding rock mass.

## Results

### *Hydrogeological characterization and resulting conceptual model*

The study area has a temperate continental climate, characterized by a mean annual temperature of 11.3° C in the city of Domodossola (Federici et al., 1967) and by mean annual rainfall in the range of 1250-2600 mm/year on the modelled area (variations are mainly related to topographic elevations).

Two rainfall maxima occurs every year: the first one in May (with values higher than 152 mm) and the second in October/November (more than 110 mm).

The water surplus on the modelled area has been calculated in the range of 700-1400 mm/year.

The resulting conceptual model evidences a groundwater flow mainly controlled by gravity and a general aquitard behaviour of rock masses (mainly gneissic formations), except for situations of tectonization, fracturation or dissolution: the main aquifers are represented by metalimestones.

The spring survey puts in evidence an higher density of springs with significant flow rates in the Crodo area and in the Alfenza valley (Fig. 6a).

Springs present flow rates in a wide range: from 0.06 l/s (ID 21) to 35 l/s (ID 24 - Lisiel); the most represented flow rates are in the range 0.05-2.5 l/s. A clear correlation between spring flow rate and spring elevation does not occur also if three main groups can be spatially distinguished: springs located at elevations between 400 and 500 m a.s.l., with flow rates higher than 10 l/s (ID3 - Oira, ID23 - Valle Oro, ID24 - Lisiel); springs between 1100 and 1500 m a.s.l., with flow rates in the range between 5 and 10 l/s (ID10 - Flecchio, ID12 - Longio, ID15 - Alfenza nord); a third group with all the remainders, located at variable elevations, with flow rates lower than 5 l/s.

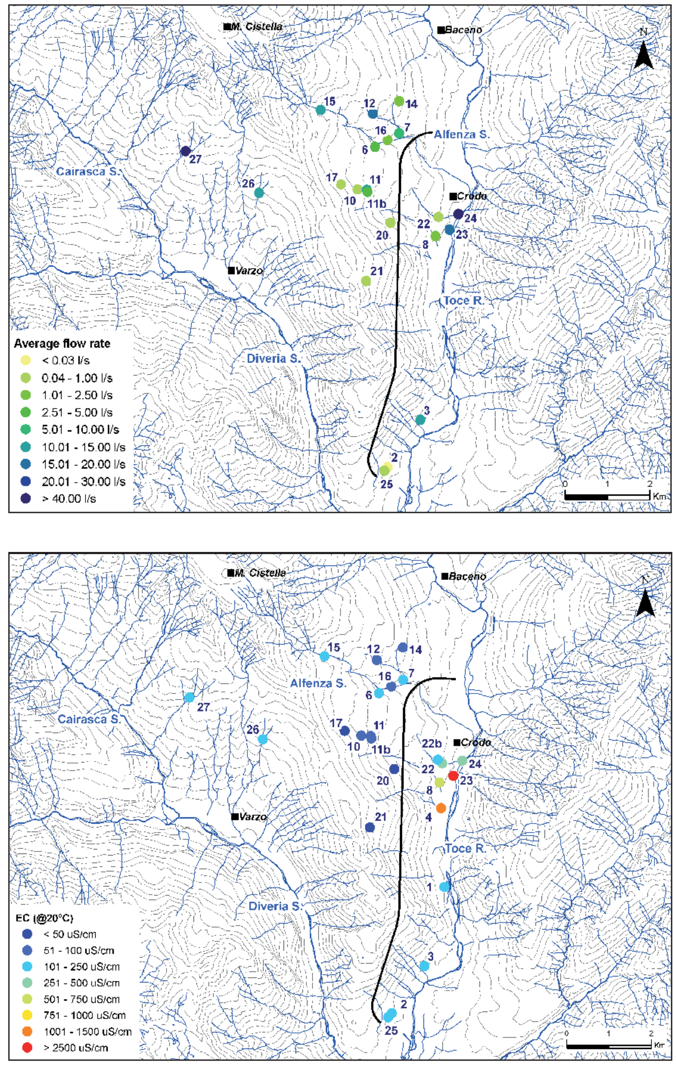


**Fig. 6:** *Location of groundwater monitoring network: a) springs ranked as a function of the average flow rate in the period Jul-05 – Jun-06; b) springs and wells ranked as a function of the average EC in the same period.*

Comparing all the available data, it can be assessed that the springs with the higher flow rates have generally a low DVI, particularly Valle Oro spring which shows a quite constant flow rate, independent from the rainfall events, and a low value of α coefficient ($6.6\ 10^{-3}\ d^{-1}$); it is representative of the end discharge of deep groundwater flow systems and recharged over a huge area.

As in nearby areas (Martinotti, 1993), three hydrochemical water types occur in the study area (Fig. 7a): $Ca\text{-}HCO_3$ facies, representative of relatively short and shallow flow pathlines circulating inside gneiss rock masses or quaternary deposits, as for example the case of Alfenza springs; $Ca\text{-}SO_4$ facies, representative of deep groundwater flow pathlines inside gypsum and/or anhydrites contained inside metalimestones (as demonstrated by the enrichment in sulphates), i.e. Valle Oro spring and Molinetto well; a $Ca\text{-}HCO_3\text{-}SO_4$ facies, that comes from the mixing of the other two.

This classification is confirmed by the groundwater mineraliza-

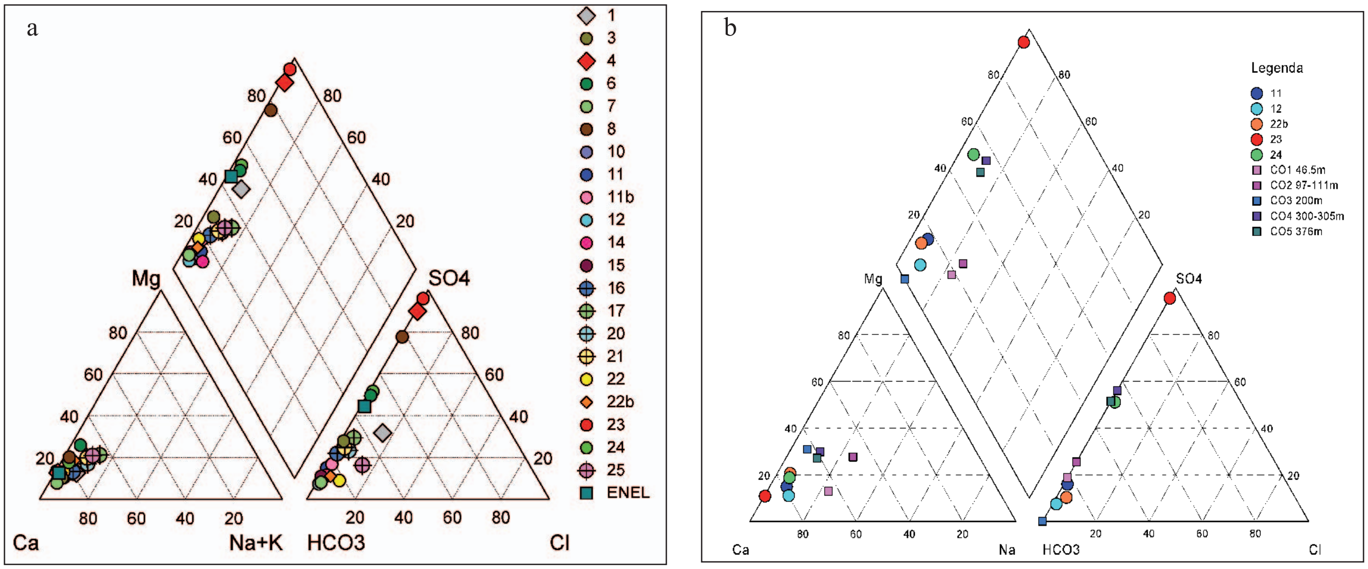


**Fig.7:** *Piper diagrams: a) all monitoring points in the study area; b) five groundwater samples collected inside borehole S3 compared with the four main monitored springs.*

tion degree, that can be inferred from the specific electrical conductivity (EC), represented in Figure 6b. A further coherent information derives from the analyses of groundwater samples collected inside boreholes at different depths: as represented in Figure 7b the two deepest samples collected inside S3 borehole (respectively $CO_4$ at 300 and $CO_5$ at 370 m b.g.l.) have the same facies of Lisiel spring.

Isotopic composition of groundwater reflects quite well the literature data (Martinotti, 1993; Martinotti et al., 1999; Pastorelli et al., 2001): the local meteoric line (Fig. 8a) is very similar to the global meteoric water line of Craig (1961). No significant thermal process occurs because no shifts in $\delta^{18}O$‰ occur. Data fall inside a small $\delta^{18}O$‰ range, but the distribution is significant: Cesa well corresponds to the shallower and shorter flow path lines and to the lower elevation of recharge areas, so characterized by the minor isotopic deplenishment; Flecchio spring is similar to Cesa well but located upstream and recharged at higher elevations; Valle Oro spring is

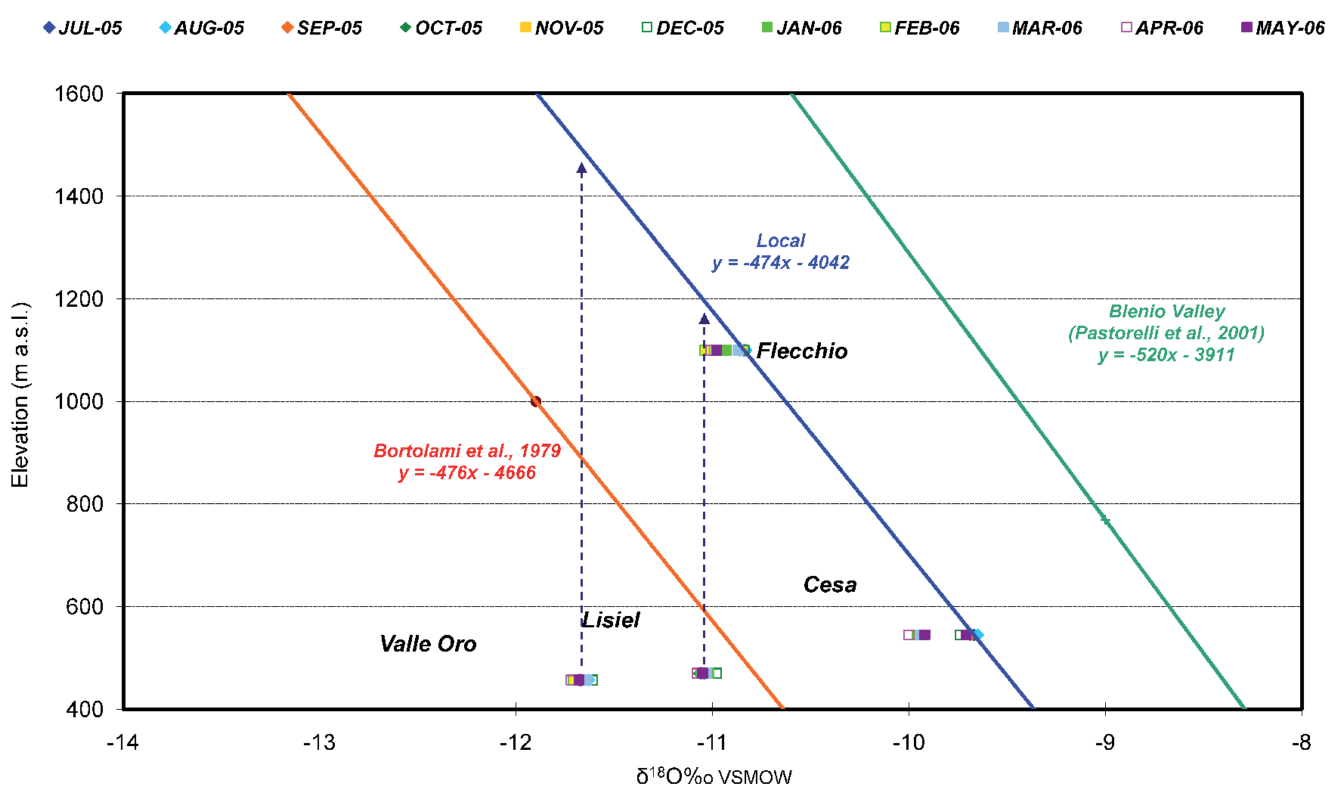


**Fig. 8a:** *Local meteoric water line derived from all the available data on the study area.*


DOI 10.4409/Am-021-10-0017

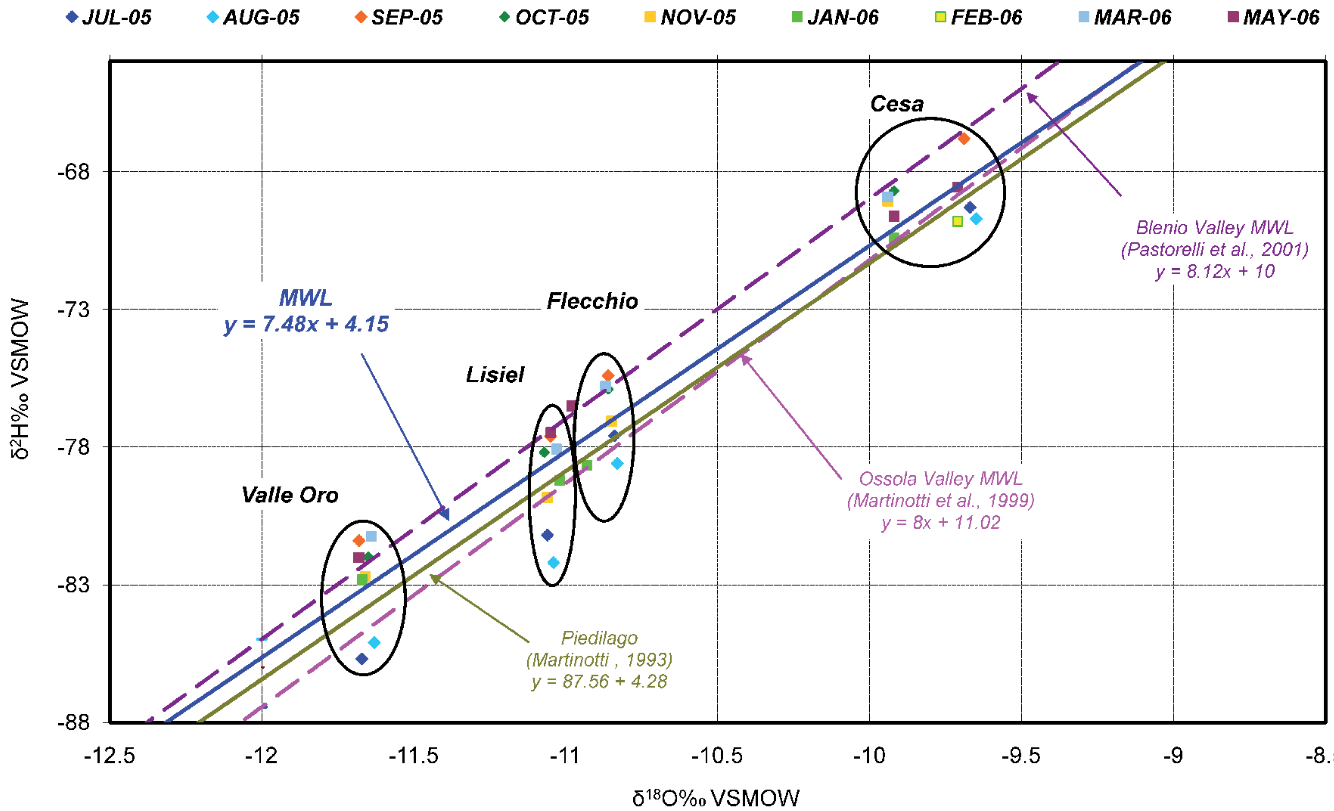


**Fig. 8b:** *Relation between spring elevation and* $\delta^{18}O$‰.

characterized by the most deplenished waters and the highest difference between theoretical recharge area average elevation and spring elevation (Fig. 8b), as it represents the discharge of deep and long flow path lines.

## Risk evaluation results from parametric methods

The final result in terms of Potential Inflow (PI), expressed as probability between 0 and 100%, for the entire tunnel is presented in Figure 9. Most critical sectors are those between 6+062 and 6+864 km, located below DSGD, where PI value (between 40-60% and 60-80%) is mainly controlled by FF (RQD), with a rating of 0.75. Other critical sectors are 177 and 178 (km 8+867 – 8+917) where the high rating of RQD index, OV (around 120 m) and K contribute to increase the PI value. The remainder of the tunnel shows PI values in the range 0 - 40 %.

The final results according to Cesano method in terms of major and minor inflows are shown respectively in Figure 10 and Figure 11. The most critical sectors for major inflows, with values between 80 and 100%, are related to lineaments occurrence and to the location of ground surface and bedrock troughs. Concerning dripping and minor inflows, the most critical sectors are located in the northern half of the tunnel where in some sector the maximum value of 100% probability is attained.

Observing Figure 9 and Figure 10 and trying to compare the results of the two methods, it's evident that PI value distribution along the tunnel is quite diversified. On average lower PI values are produced by Dematteis method. Nevertheless the authors consider more reliable these results, for two reasons: it is more codified than Cesano method in the involved geological framework and it is strongly based on rock mass intrinsic parameters. Cesano method for major inflows

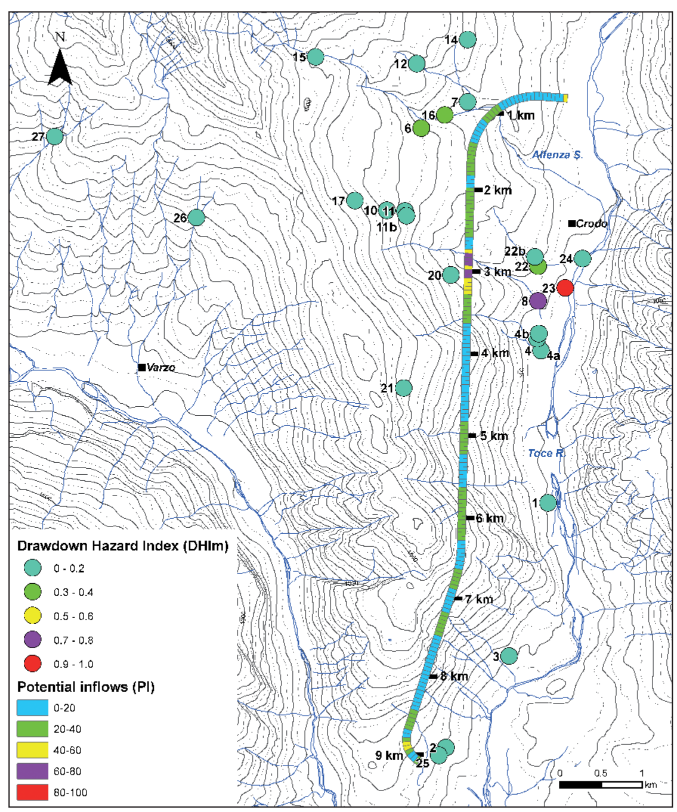


**Fig. 9:** *Potential inflows inside the tunnel according to Dematteis method and modified Drawdown Hazard Index (DHIM) at the water point (springs and wells).*

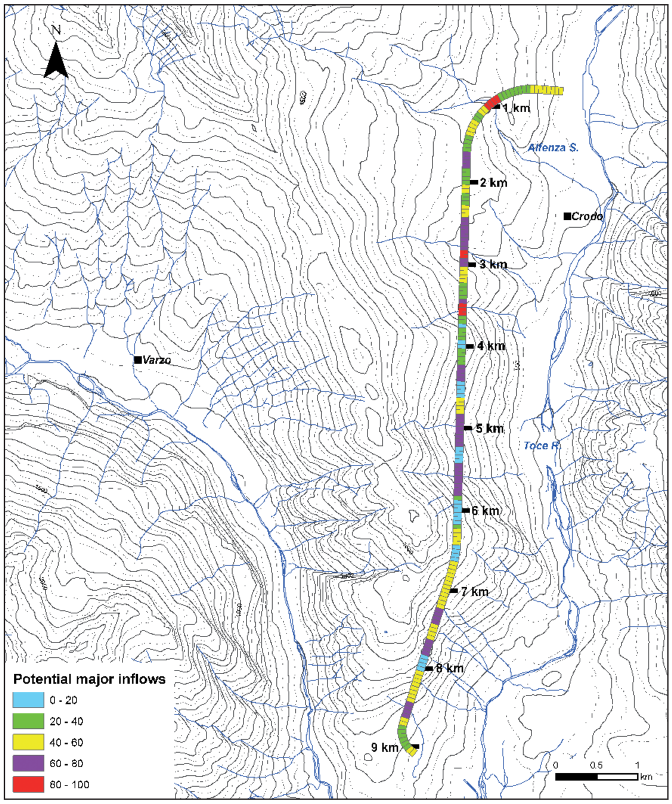


**Fig. 10:** *Potential major inflows inside the tunnel according to Cesano method.*

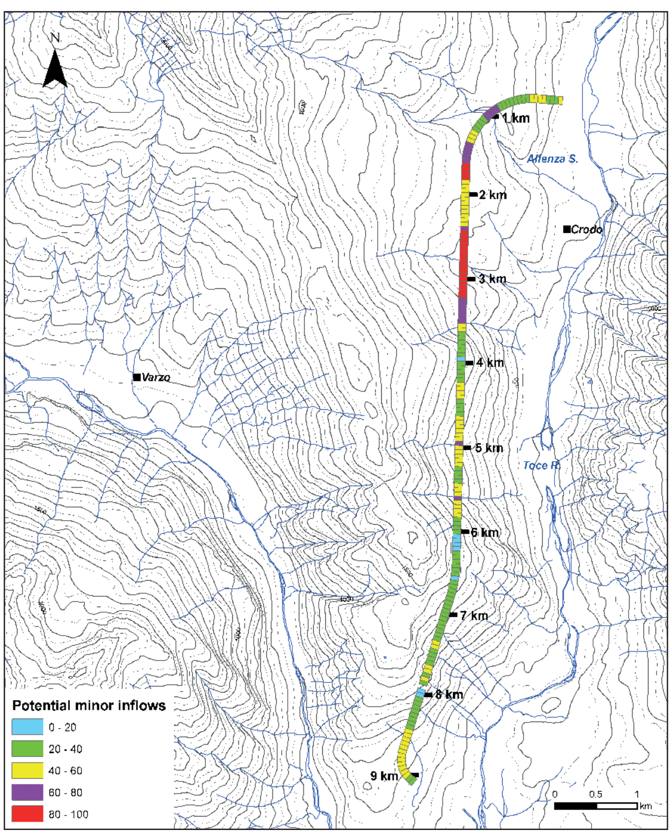


**Fig.11:** *Potential minor inflows inside the tunnel according to Cesano method.*

prediction mainly takes into account morphological and geological factors, which cannot play a key role with such a thick overburden as occurring in the investigated site.

Frequency histogram for Dematteis PI (Fig. 12) is typically log-normal, as should be if we consider the output of a combination of hydrogeological factors; modal class corresponds to a very low PI value (15%) as usually observed for actual drainage distribution occurrence in bored tunnels (Masset & Loew, 2010). In hard rock aquifers big inrushes are sporadic and scattered drainage events are rare with respect to diffuse groundwater drops falling down from the excavated tunnel surface (Gargini et al., 2008). Also for this reason Dematteis output appears more reliable than Cesano method output.

DHI value for all springs (and for the 5 wells, considered as water-point potentially subject to impact), according the application of Dematteis method, is reported in Table 7 as DHID; it is important to emphasize that DHID never results as "0", being conditioned by PI value, always higher than 0.23. So it never happens that there is no DHI probability occurrence. Springs with higher DHI value are ID 23 (Valle Oro; 0.91 DHI) and ID 8 (Vegno; 0.68 DHI), both located near a main fault crossing the tunnel and connected to deep groundwater flow systems.

If DHID values are ranked in classes based on the limits proposed originally by Dematteis method (Table 1), then only 1 spring occurs in classes 1 and 2 (respectively Valle Oro and Vegno), whereas the remainders 19 springs and 5 wells fall in the "partial risk" class (DHID >0.23). Among these, 10 springs (and 1 well, Sarizzo Well) resulted with a minimum DHID value equal to 0.23; as already mentioned a value of 0.23 derives simply from the fact that PI is always positive. This consideration shows a limit of the methodology: also a spring located quite far from the tunnel path, connected to a shallow groundwater flow system and not related to any tectonic lineament, e.g. a receptor with very low vulnerability (if any), will receive however a not fair DHID value, being quite important the control of PI. If PI value is high, accordingly DHID value will be at least medium for all springs involved in the evaluation. For this reason Dematteis method tends to overestimate impact risk for springs with low hydrogeological vulnerability to impact; the DHID estimation is more reliable for medium-high vulnerability receptors.

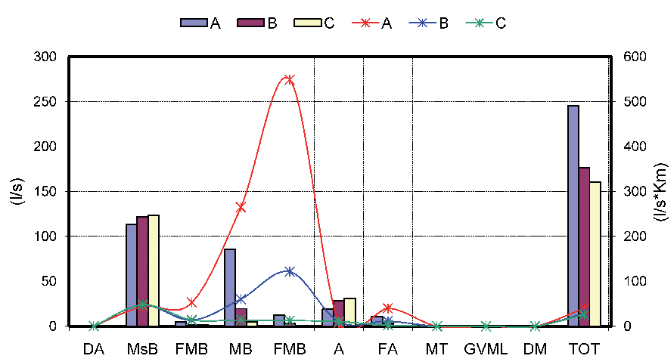


**Fig.12:** *Total forecasted tunnel outflow (bars, left scale) and specific outflow normalized on distance (line, right scale) in relationship to lithology (DA = Quaternary fluvial deposits, MsB = Baceno Micascists, FMB = Fault zones in Baceno Micascists, MB = Baceno Metasediments, FMB = Fault zones in Baceno Metasediments, A = Antigorio Gneiss, FA = Fault zones in Antigorio Gneiss, MT = Teggiolo Metasediments, GVML = Valgrande and Monte Leone Gneiss, DM = Glacial deposits, TOT = Total).*

 DOI 10.4409/Am-021-10-0017

Taking into account these limitations and considering other improvements of hydrogeological nature based on previous experiences derived from tunnel drilled in hard rock aquifers, the final index of drawdown has been slightly modified by defining a new index called "modified DHI" (DHIM; Table 6). DHIM was evaluated in the same manner of DHID with the following rules:

1) If the tunnel-spring Euclidean distance is more than 1000 m and there is no evidence of hydrogeological connection with the tunnel, DHID is assumed equal to 0, notwithstanding the PI value; this consideration is based on the results of the hydrogeological monitoring of the springs and wells along the pathway of Florence-Bologna high speed railway tunnel connection (Canuti et al., 2009);

2) If the tunnel-spring Euclidean distance is lower than 1000 m and there is no evidence of hydrogeological connection with the tunnel, DHID is assumed to be based on the average PI relative to a tunnel sector included in a buffer sphere with radius 1000 m and centred at the spring;

3) If the tunnel-spring Euclidean distance is lower than 1000 m and there is evidence of hydrogeological connection with the tunnel, two separate buffer zones are considered: a sphere of 1000 m radius centred at the spring and a 400 m long tunnel sector across the intersection fault-tunnel; the highest value of PI between these buffer zones is chosen, conservatively, to calculate DHI at the spring;

4) If the tunnel-spring Euclidean distance is higher than 1000 m and there is evidence of hydrogeological connection with the tunnel (with a total distance of connection along faults minor than 2000 m), a 400 m long tunnel sector buffer zone across the intersection fault-tunnel is defined for the evaluation of the PI;

5) DHI value so obtained is normalized to 1 and all the entire value range is ranked according 5 classes regularly spaced between 0 and 1. The normalized DHI value is called modified DHI (DHIM).

The final result in terms of DHIM for the whole set of receptors is shown in the map of Fig. 9. The comparison between DHID and DHIM class ranking is put in evidence in Table 7.

### *Tunnel inflows and springs dewatering forecasted with the numerical model*

The numerical simulations with the tunnel completely draining forecast piezometric drawdowns in the range of 200-800 m, depending on the K values assigned to the plastic zone around the tunnel. For all the simulations the highest drawdown occurs above the tunnel at the big curve close to the northern entrance (around km 1) and decreases progressively from north to south in the longitudinal direction of the tunnel; the drawdown stops where the tunnel elevation is higher than the piezometric surface in natural conditions. In the transversal direction (W-E) the depressurization effect progressively decreases moving away from the tunnel axis and disappears at a maximum distance of about 5 km on the west side.

In all the three simulations the piezometric drawdown causes the drying up of two springs, located in the area of the maximum impact (Cesa and Vegno). At the other two springs (Lisiel and Valle Oro), located in the same area but at lower elevations than the previous ones, the model forecasts a flow rate decrease in the 4-6% range (Tab. 8).

In the three simulations the total tunnel drainage in steady-state conditions is respectively 273, 286 and 316 l/s.

The highest contribution comes from the Baceno metasediments,

**Tab. 6:** *DHI values for all springs according the application of Dematteis method; 1= highest, 5 = lowest impact probability.*

| ID | Name | $DHI_D$ | $DHI_D$ CLASS | $DHI_M$ | $DHI_M$ CLASS |
|---|---|---|---|---|---|
| 1 | SARIZZO WELL | 0.23 | 3 | 0 | 5 |
| 2 | BISOGNO | 0.23 | 3 | 0.11 | 5 |
| 10 | FLECCHIO ALTA | 0.23 | 3 | 0 | 5 |
| 11 | FLECCHIO | 0.23 | 3 | 0.14 | 5 |
| 11b | FLECCHIO ISOLATA | 0.23 | 3 | 0.13 | 5 |
| 15 | ALFENZA NORD | 0.23 | 3 | 0 | 5 |
| 17 | CAVORAGA - FAIO' | 0.23 | 3 | 0.198 | 5 |
| 21 | CHEGGIO | 0.23 | 3 | 0 | 5 |
| 25 | LA CONCA | 0.23 | 3 | 0.11 | 5 |
| 26 | LA ROCCA | 0.23 | 3 | 0 | 5 |
| 27 | CALANTAGINE | 0.23 | 3 | 0 | 5 |
| 24 | LISIEL | 0.34 | 3 | 0 | 5 |
| 3 | OIRA | 0.46 | 3 | 0.07 | 5 |
| 4 | MOLINETTO 1 | 0.46 | 3 | 0.09 | 5 |
| 4a | MOLINETTO 2 | 0.46 | 3 | 0.13 | 5 |
| 4b | MOLINETTO 3 | 0.46 | 3 | 0.14 | 5 |
| 6 | VICENO | 0.46 | 3 | 0.31 | 4 |
| 7 | LA VALLE | 0.46 | 3 | 0.08 | 5 |
| 12 | LONGIO | 0.46 | 3 | 0.16 | 5 |
| 14 | TRONA | 0.46 | 3 | 0.16 | 5 |
| 16 | ALFENZA SUD | 0.46 | 3 | 0.22 | 4 |
| 22 | CESA INFERIORE | 0.46 | 3 | 0.37 | 4 |
| 22b | CESA WELL | 0.46 | 3 | 0.18 | 5 |
| 8 | VEGNO | 0.68 | 2 | 0.75 | 2 |
| 23 | VALLE ORO | 0.91 | 1 | 1 | 1 |
| 20 | RONCONI | 0.55 | 3 | 0.6 | 3→5 |

**Tab. 7:** *Impacts on springs forecasted by means of MODFLOW simulations with the draining tunnel and with the 3 different K values for the plastic zones.*

| | Lisiel (24) | Valle Oro (23) | Vegno (8) | Cesa (22) | |
|---|---|---|---|---|---|
| **Observed** | 34.96 | 19.97 | 1.55 | 0.2 | Q (l/s) |
| **Ante-operam** | 34.96 | 19.97 | 1.5 | 0.2 | Q (l/s) |
| **Post (1/2 order)** | 33.56 | 18.92 | 0 | 0 | Q (l/s) |
| | 4.00 | 5.25 | 100 | 100 | deficit % |
| **Post (1 order)** | 33.47 | 18.9 | 0 | 0 | Q (l/s) |
| | 4.25 | 5.39 | 100 | 100 | deficit % |
| **Post (2 order)** | 33.37 | 18.82 | 0 | 0 | Q (l/s) |
| | 4.53 | 5.77 | 100 | 100 | deficit % |
| **Average deficit** | **4.26** | **5.47** | **100** | **100** | deficit % |

which produce flow rates in the range of 100-115 l/s (that is in the range 31.6-42% of the total drainage). Progressively minor contributions come from the remainder hydrogeological units and related fault zones: Baceno micaschists, fault zones in Baceno metasediments, fault zones in Antigorio Gneiss, Antigorio Gneiss and fault zones in Baceno micaschists (Tab. 9).

Considering the inflow normalised by meters of tunnel, the sectors crossing the faults in Baceno metasediments present the highest values, from 0.833 to 1.215 l/s*m; these values progressively decrease in the following order: Baceno metasediments, fault zones in Baceno micaschists, Baceno micaschists, fault zones in Antigorio Gneiss and Antigorio Gneiss. These results mainly derive from the assigned hydraulic conductivities values but also from the geometric position of the units with respect to the piezometric surface and the tunnel alignment.

In the three simulations of the dispersant tunnel (with an inner flow rate of 18 $m^3/s$), the tunnel still has a draining behavior where located below the piezometric surface, while it recharges the aquifer where located above the piezometric surface.

This leads to a small decrease in terms of depressurization effects in the area of the highest impact; at springs Lisiel and Valle Oro flow rates increase of 0.01 and 0.28 l/s with respect to the simulations with the draining tunnel, while at springs Vegno and Cesa the impact is the same (Tab. 10).

Finally, the last three simulations, with impermeable linings in the most permeable tunnel reaches, demonstrate that linings effectively reduce the depressurization in terms of intensity and area of influence. Along the tunnel maximum drawdowns decrease of more than a half with respect to the corresponding values calculated in the first simulation with the tunnel completely draining (~350 m of drawdown), resulting respectively in: 153 m for the A, 140 m for the B, and 138 m for the C scenario. The flow rates at springs Lisiel and Valle Oro decrease respectively of 2% and 4.5% respect to the natural conditions values. Cesa spring remains completely impacted in all the scenarios, while Vegno spring gets completely dried up only in the A scenario, while in the B and C scenario presents a flow rate decrease respectively of 82% and 64% with respect to the natural conditions values (Tab. 11). The total tunnel drainage decreases significantly too: 245 l/s (A), 176 l/s (B) and 161 l/s (C).

The general effect of tunnel sealing results quite good, even if it increases the drainage from the tunnel reaches without linings, due to the higher hydraulic gradient (Tab. 12 and Fig. 12).

## *Comparison between the two methods*

Before to comment upon a comparison between parametric and numerical modelling approach it should be noted that both evaluations of tunnel impact are based on a detailed build-up of the geological model and on a dedicated geological survey. Such a site specific direct survey is the essential prerequisite for a reliable impact evaluation, whatever is the chosen approach.

In every approach the conservativity principle was always followed, e.g. sizing the thickness of Plastic Zone or modelling at steady state conditions.

On the other side, the reliability of forecasted scenarios is limited by the calibration data-set (hydraulic head and springs monitoring and pumping tests data).

In Table 12 the final results in terms of tunnel impact forecast are reported. The impact scenario is relative to the draining tunnel at steady state conditions. The resulting risk classes represent the probability and the severity of impact occurrence from, respectively, the parametric (DHIM evaluation) and the numerical evaluation process.

Four risk classes are evidenced in colour from red (class I) to blue (class IV); in the third column of Table 12 the final output of the integrated tunnel impact evaluation is shown. Final choice was based as follows: if, for a given spring, parametric and numerical method produce 2 risk classes separated by an intermediate class, this last one is assigned as final output, recognizing an equal degree of uncertainty to both methods; if parametric and numerical method produce 2 contiguous risk classes for the same spring, the worst one is assigned as final output, for the principle of conservativity.

The excavation and consequent drainage of Crevola Toce diversion tunnel will configure the following most expected scenarios of impact against main hydrogeological receptors:

- medium risk for Valle Oro spring: very high probability (91%) of a 5% depletion of average annual flow rate (risk is ranked as medium because probability is high, according DHIM output, but discharge depletion is poor);
- medium risk for Vegno spring: high probability (68%) of a 31% depletion of discharge;
- medium risk for Cesa spring: medium probability (46%) of complete drying up;
- medium-low risk for Lisiel spring: low probability (34%) of a 6% discharge depletion;

 DOI 10.4409/Am-021-10-0017

**Tab. 8:** *Tunnel inflows forecasted by MODFLOW simulations, according to the 3 scenarios described in the main text; tunnel reaches crossing the different hydrogeological units have been distinguished in order to calculate linear flow rates (every m or km of tunnel advancement).*

| **Zone Budget** | **Hydrogeological Unit** | **Post (1/2 order)** | | **Post (1 order)** | | **Post (2 order)** | |
|---|---|---|---|---|---|---|---|
| | | **Q (l/s)** | **Q (l/s*Km)** | **Q (l/s)** | **Q (l/s*Km)** | **Q (l/s)** | **Q (l/s*Km)** |
| 6 | Quaternary fluvial deposits | 0 | 0 | 0 | 0 | 0 | 0 |
| 7 | Baceno micaschists | 90.83 | 35.05 | 105.01 | 40.52 | 155.81 | 60.12 |
| 8 | Fault in Baceno micaschists | 14.44 | 164.91 | 14.58 | 166.44 | 15.99 | 182.51 |
| 9 | Metasediments (Baceno syncline) | 114.84 | 356.15 | 116.57 | 361.54 | 100.08 | 310.38 |
| 10 | Fault in Metasediments (Baceno syncline) | 27.61 | 1214.81 | 23.8 | 1047.26 | 18.94 | 833.31 |
| 11 | Antigorio gneiss | 12.5 | 4.39 | 12.85 | 4.63 | 13.08 | 4.76 |
| 12 | Fault in Antigorio gneiss | 12.75 | 46.17 | 12.82 | 46.43 | 12.33 | 44.62 |
| 13 | Metasediments (Teggiolo syncline) | 0 | 0 | 0 | 0 | 0 | 0 |
| 14 | Valgrande and Monte Leone gneiss | 0 | 0 | 0 | 0 | 0 | 0 |
| 15 | Quaternary glacial deposits | 0 | 0 | 0 | 0 | 0 | 0 |
| | Total and average | **272.97** | **44.2** | **285.64** | **46.82** | **316.22** | **52.04** |

**Tab. 9:** *Impacts on spring flow rates forecasted by model simulations with the draining tunnel (Post) and dispersant tunnel (Stream).*

| | **Lisiel (24)** | **Valle Oro (23)** | **Vegno (8)** | **Cesa (22)** | |
|---|---|---|---|---|---|
| **Observed** | 34.96 | 19.97 | 1.55 | 0.2 | Q (l/s) |
| **Ante-operam** | 34.96 | 19.97 | 1.5 | 0.2 | Q (l/s) |
| **Stream (1/2 order)** | 33.75 | 19.07 | 0 | 0 | Q (l/s) |
| | 3.46 | 4.54 | 100 | 100 | deficit % |
| **Stream (1 order)** | 33.6 | 19 | 0 | 0 | Q (l/s) |
| | 3.87 | 4.90 | 100 | 100 | deficit % |
| **Stream (2 order)** | 33.45 | 18.83 | 0 | 0 | Q (l/s) |
| | 4.30 | 5.72 | 100 | 100 | deficit % |
| | 3.88 | 5.05 | 100 | 100 | average deficit % |

**Tab. 10:** *Impacts on spring flow rates forecasted by model simulations with the draining tunnel (Post 1 order) and with the sealed tunnel (linings where the major forecasted groundwater inflows, see the main text for more detail).*

| | **Lisiel (24)** | **Valle Oro (23)** | **Vegno (8)** | **Cesa (22)** | |
|---|---|---|---|---|---|
| Observed | 34.96 | 19.97 | 1.55 | 0.2 | Q (l/s) |
| Ante-operam | 34.96 | 19.97 | 1.5 | 0.2 | Q (l/s) |
| Post 1 order | 33.56 | 18.92 | 0 | 0 | Q (l/s) |
| | 4.00 | 5.25 | 100 | 100 | deficit % |
| A scenario | 33.73 | 19.07 | 0 | 0 | Q (l/s) |
| | 3.52 | 4.52 | 100 | 100 | deficit % |
| B scenario | 34.12 | 19.39 | 0.27 | 0 | Q (l/s) |
| | 2.38 | 2.90 | 82.10 | 100 | deficit % |
| C scenario | 34.23 | 19.48 | 0.55 | 0 | Q (l/s) |
| | 2.09 | 2.46 | 63.64 | 100 | deficit % |
| | 2.66 | 3.29 | 81.91 | 100 | average deficit % |

**Tab. 11:** *Tunnel inflows forecasted by MODFLOW simulations, according to the 3 scenarios with the sealed tunnel (as described in the main text); tunnel reaches crossing the different hydrogeological units have been distinguished in order to calculate linear flow rates (every km of tunnel advancement).*

| Zone Budget | Hydrogeological Unit | Scenario A | | Scenario B | | Scenario C | |
|---|---|---|---|---|---|---|---|
| | | Q (l/s) | Q (l/s*Km) | Q (l/s) | Q (l/s*Km) | Q (l/s) | Q (l/s*Km) |
| 6 | Quaternary fluvial deposits | 0 | 0 | 0 | 0 | 0 | 0 |
| 7 | Baceno micaschists | 113.18 | 43.67 | 121.84 | 47.01 | 123.4 | 47.62 |
| 8 | Fault in Baceno micaschists | 4.58 | 52.28 | 1.17 | 13.31 | 1.2 | 13.75 |
| 9 | Metasediments (Baceno syncline) | 85.32 | 264.61 | 19.33 | 59.93 | 4.43 | 13.74 |
| 10 | Fault in Metasediments (Baceno syncline) | 12.47 | 548.63 | 2.75 | 121.06 | 0.28 | 12.37 |
| 11 | Antigorio gneiss | 18.87 | 6.5 | 28.22 | 9.48 | 30.66 | 10.22 |
| 12 | Fault in Antigorio gneiss | 10.91 | 39.51 | 3.03 | 10.97 | 0.56 | 2.01 |
| 13 | Metasediments (Teggiolo syncline) | 0 | 0 | 0 | 0 | 0 | 0 |
| 14 | Valgrande and Monte Leone gneiss | 0 | 0 | 0 | 0 | 0 | 0 |
| 15 | Quaternary glacial deposits | 0 | 0 | 0 | 0 | 0 | 0 |
| | **Total and average** | **245.33** | **39.4** | **176.33** | **27.98** | **160.54** | **25.38** |

**Tab. 12:** *Spring forecasted impact scenarios according to the parametric (DHI) and numerical (MODFLOW) models. See text for the explanation of the different global risk classes definition.*

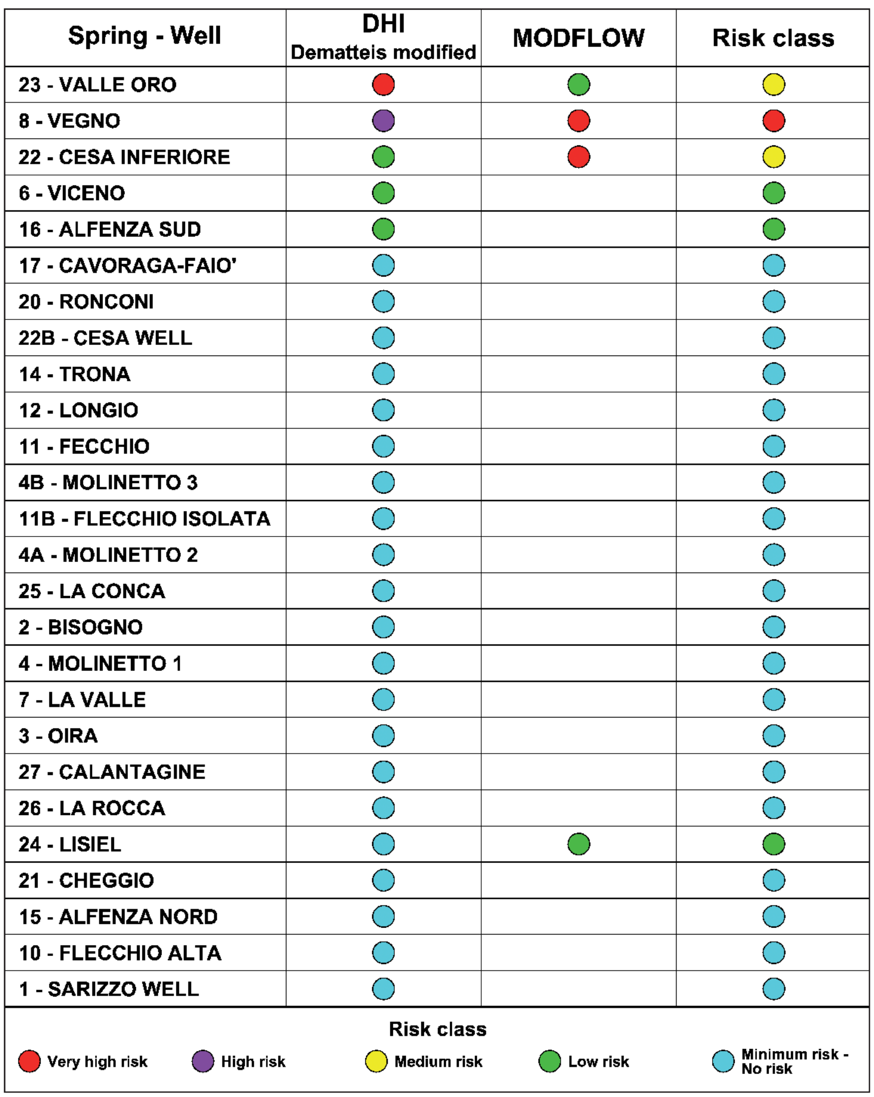


 DOI 10.4409/Am-021-10-0017

• medium-low risk for Molinetto wells: medium probability (46%) of well yield depletion;

• medium-low risk for the following springs: Oira, Viceno, La Valle, Trona, Alfenza Sud, Longio and for Cesa well: medium probability (46%) of impact;

• low risk for the remainder of receptors: low impact probability (23%) with shallow groundwater flow systems. Also Ronconi spring was assigned to this last class, independently from the DHIM output, because representative of a shallow groundwater flow system located at elevations much higher than tunnel.

## Conclusions and remarks

An evaluation method of tunnel drainage impact risk against hydrogeological receptors has been presented and discussed. In order to overcome the intrinsic uncertainty of a forecasting process in ante-operam conditions and to strengthen the evaluation, a rating and weighting parametric method and a numerical model have been used contemporarily; their results have been compared and a final forecasting resulted from their arrangement with a conservativity approach.

The two methods evidenced their respective limits and advantages. Parametric methods do not take into account the groundwater flow equation, but allow to assess quite easily a risk probability for all the springs; another advantage is that they can be adapted to the case study, as a function of the available input data; anyway the rough results need a critical evaluation and refinement. On the other side, numerical modelling requires more data (hydraulic heads and flows) and its reliability depends a lot on data quantity and quality and on the goodness of calibration process; but the modelling process allows to check the conceptual model by applying the groundwater flow equation.

In the specific case study, the peculiarity and the strength of the available data set was the use of different field methods (geological surveys, flow and piezometric measurements, hydrochemistry, isotopic techniques), helping a lot in the the conceptual model set up. The data set was sufficiently detailed for the application of parametric methods, but still scarce for the numerical modelling process. Furthermore, the model set up required a strong effort due to the geological complexity and the steep slopes.

The experience made with the here presented case study suggests to use firstly parametric methods as a "first level" risk evaluation on all the water points, in order to assess the most vulnerable water points; then, on these vulnerable points a "second level" risk evaluation should be developed consequently by means of numerical modelling, based on a more detailed hydrogeological data set.

**Acknowledgment:** Presented at Session "Hydrogeological impacts of tunnels", GEOITALIA 2009, Rimini, September 2009 (session's conveners: Alessandro Gargini, Valentina Vincenzi, Michele Sapigni).

## References

Aller L., Bennett T., Lehr J.H., Petty R.J. (1985) - DRASTIC - a standardized system for evaluating ground water pollution potential using hydrogeologic settings: U.S. Environmental Protection Agency, Robert S. Kerr Environmental Research Laboratory, Office of Research and Development, EPA/600/2–85/018, 163 pp.

Astolfi G., Sapigni M. (1999) - Impianto Crevola Toce III - Progetto di Massima - Relazione geologica. Enel Spa, internal report.

Barton C.M. (1974) - Engineering classification of rock masses for the design of tunnel support. Rock Mechanics, 6, 4, pp.189-239.

Bigioggero B., Boriani A., Origoni Giobbi E. (1977) - Microstructure and mineralogy of an Orthogneiss (Antigorio Gneiss - Lepontine Alps). Rendiconti Società Italiana di Mineralogia e Petrologia, 33, 99-108.

Bistacchi A., Massironi M. (2000) - Post-nappe brittle tectonics and kinematic evolution of the north-western Alps: an integrated approach. Tectonophysics, 327, 267-292.

Bortolami G.C., Ricci B., Sella G.F., Zuppi G.M. (1979) - Isotope hydrology of the Val Corsaglia, Maritime Alps, Piedmont, Italy, in Isotope Hydrology 1978, Vol.I, IAEA Symposium 228, June 1978, Neuheberg, Germany, pp. 327-350.

Campani M., Mancktelow N., Seward D., Rolland Y., Müller W., Guerra I. (2010) - Geochronological evidence for continuous exhumation through the ductile-brittle transition along a crustal-scale low-angle normal fault: Simplon Fault Zone, central Alps. Tectonics, 29, TC3002, doi:10.1029/2009TC002582.

Canuti P., Ermini L., Gargini A., Martelli L., Piccinini L., Vincenzi V. (2009) - Le gallerie TAV attraverso l'Appennino toscano: impatto idrogeologico ed opere di mitigazione. Edifir-Edizioni Firenze, Firenze, pp. 207.

Castiglioni G.B. (1958) - Studio geologico e morfologico del territorio di Baceno e Premia. Memorie degli Istituti di Geologie e Mineralogie dell'Università di Padova, vol. XX, 2-82.

Cesano D., Olofsson B., Bagtzoglou (2000) - Parameters regulating groundwater inflows into hard rock tunnels-a statistical study of the Dolmen tunnel in southern Sweden. Tunneling and underground Space Technology, V. 15/2, p. 153-165

Civita M. (1973) - Schematizzazione idrogeologica delle sorgenti normali e delle relative opere di captazione. In Memorie e Note Ist. Geol. Aplplic. Napoli, 12, 1973, pp.1-34.

Civita M., De Maio M. (2000) - Valutazione e cartografia automatica degli acquiferi all'inquinamento con il sistema parametrico SINTACS R5. Pitagora Editore, Bologna, 275pp.

Civita M. (2005) - Idrogeologia applicata e ambientale, Casa Editrice Ambrosiana, pp 331-336.

Civita M., Gargini A., Pranzini G. (1999) - Metodologia di redazione della carta della vulnerabilità intrinseca e del rischio di inquinamento degli acquiferi del Valdarno Medio. Quaderni di Geologia Applicata, 2, VOL.1, pp. 1.59-1.73.

Clark I., Fritz P. (1997) - Environmental Isotopes in Hydrogeology, CRC Press LLC.

Craig H. (1961) - Isotopic variations in meteoric waters. Science, 133, pp. 1702-1703.

Deere, D.U., Deere, D.W. (1989). - Rock Quality Designation (RQD) After Twenty Years - Technical Report GL-89-1, U.S. Army Engineer Waterways Experiment Station, Vicksburg, MS 39180.

Deere, D.U., Merritt, A.H., Coon, R.F. (1969). - Engineering Classification Of In Situ Rock - Air Force Systems Command, Kirtland Air Force Base, Report AFWL-64-144.

Dematteis A., Kalamaras G., Eusebio A. (2001) - A system approach for evaluating springs drawdown due to tunneling - AITES-ITA 2001 World Tunnel Congress: Progress in tunnelling after 2000 – p. 257-264. Milano, 10-13 June 2001

Domenico P., Schwartz F. (1998), - Physical and chemical Hydrogeology, second edition. John Wiley & Sons, Inc., New York, USA

Einstein H.H. (1988) - Special lecture: landslide risk assessment procedure" - Atti di "V International Symposium on Landslides, Losanna, 2, pp.1075-1090.

Federici P.C., Saccani F., Parietti P., 1967 - Le acque salutari della Val d'Ossola, collana di monografie dell'ateneo parmense, n. 18.

Federico F. (1984) - Il processo di drenaggio da una galleria in avanzamento - Rivista Italiana di Geotecnica, V.4, p. 191-208.

Gargini A., Piccinini L., Martelli L., Rosselli S., Bencini A., Messina A., Canuti P. (2006) - Idrogeologia delle unitá torbiditiche: un modello concettuale derivato dal rilevamento geologico dell'Appennino Tosco-Emiliano e dal monitoraggio ambientale per il tunnel alta velocità ferroviaria Firenze-Bologna - Bollettino Società Geologica Italiana, 125 (2006), 293-327.

Goodman R.E., Moye D., Schalkwyk A., Javandel I. (1965) - Groundwater inflows during tunnel driving.- Geol. Soc. America Publication – Engneering Geology, V. 2, p. 39-56.

Grasemann B., Manktelow N. (1993) - Two-dimensional thermal modelling of normal faulting: the Simplon Fault Zone, Central Alps, Switzerland. Tectonophysics, 225, 155-165.

Grosjean G., Sue C., Burkhard M. (2004) - Late Neogene extension in the vicinity of the Simplon fault zone (central Alps, Switzerland). Eclogae geol. Helv., 97; 33-46.

Harbaugh A.W., Banta E.R., Hill M.C., Mcdonald G. (2000) - MODFLOW-2000, The U.S. Geological Survey modular ground-water model - User Guide to modularization concepts and the ground-water flow process - U.S. Geological Survey, Open-File Report 00-92

Kanit T., Forest S., Galliet I., Mounoury V., Jeulin D. (2003) - Determination of the size of the representative volume element for random composites: statistical and numerical approach. International Journal of Solids and Structures, 40, 3647–3679.

Jiao Y., Hudson J.A. (1995) - The Fully-Coupled Model for Rock Engineering Systems. - International Journal of Rock Mechanics and Mining Sciences & Geomechanics Abstracts, 32, (5), 491-512. Oxford, United Kingdom: Elsevier Science)

Lei S. (1999). - An analytical solution for steady state flow into a tunnel." Ground Water - V. 37/1, p. 23-26.

Lei S. (2000). - Steady state flow into a tunnel with constant pressure boundary. - Ground Water V.38/5, p. 643-644.

Leopold L. B. Et Al. (1971) - A procedure for evaluating environmental impact, U.S. Geological Survey Circular 645, Washington D.C., U.S. Dep. Of the Interior.

Loew S. (2002) - In Barla G. & Barla M. (Eds.) - Le opere in sotterraneo e il rapporto con l'ambiente - IX ciclo MIR, Torino 26-27 novembre 2002, Patron Editore, p. 201-217.

Long J.C.S., Remer J.S., Wilson C.R., Witherspoon P.A. (1982) - Porous Media Equivalent for Networks of Discontinuous Fractures. Water Resources Research, 18(3), 645-658.

Maillet E. (1905) - Essais d'hydraulique souterraine et fluviale. Librairie Sci. Hermann Paris, 218pp.

Mancktelow N. (1985) - The Simplon line: a major displacement zone in the western Lepontine Alps. Eclogae geol. Helv. 78, 73-96.

Martinotti G. Per Enel Produzione (1993) - Impianto di Piedilago - Studio geologico strutturale e idrologico - Rapporto finale del 30 aprile 1993.

Martinotti G., Marini L., Hunziker J C., Perello P., Pastorelli S. (1999) - Geochemical and geothermal study of springs in the Ossola-Simplon Region, in Eclogae geol. Helv. 92 (1999), pp. 295-305.

Masset O., Loew S. (2010) - Hydraulic conductivity distribution in crystalline rocks, derived from inflows to tunnels and galleries in the Central Alps, Switzerland. Hydrogeology Journal, 18, pp. 863-891.

Maxelon M., Mancktelow N. (2005) - Three-dimensional geometry and tectonostratigraphy of the Pennine zone, Central Alps; Switzerland and Northern Italy. Earth-Science Reviews, 71, 171-227.

Mcdonald M.G., Harbaugh A.W. (1988) - A Modular Three-Dimensional Finite-Difference Ground-Water Flow Model - U.S. Geological Survey, Techniques of Water-Resources Investigations, Book 6, Chapter A1

Mehl S.W., Hill M.C.,( 2001), - MODFLOW-2000, The U.S. Geological Survey Modular Ground-Water Model - User Guide to the Link-Amg (LMG) Package for Solving Matrix Equations Using an Algebraic Multigrid Solver: U.S. Geological Survey Open-File Report 01-177, 33 p.

Milnes A. G., Greller M., Müller R. (1981) - Sequence and style of major post-nappe structures, Simplon-Pennine Alps. Journal of Sructural Geology, 3, 411-420.

Mun Y., Uchrin C.G. (2004) - Development and Application of a MODFLOW Preprocessor Using Percolation Theory for Fractured Media. Journal of the American Water Resources Association, 40(1), 229-239.

Pastorelli S., Marini L., Hunziker J. (2001) - Chemistry, isotop values ($\delta$D, $\delta^{18}$O, $\delta^{34}S_{SO_4}$) and temperatures of the water inflows in two Gotthard tunnels, Swiss Alps, in Applied Geochemistry 16 (2001), pp. 633-649.

Prudic D.E. (1989) - Documentation of a computer program to simulate stream-aquifer relations using a modular, finite-difference, ground-water flow model. U.S. Geological Survey, Open-File Report 88-729.

Schmidt C., Preiswerk H. (1905) - Geologische Karte der Simplongruppe. Beiträge zur Geologischen Karte der Schweiz, [N.F.] 26, Spezialkarte No. 48.

Steck A. (2008) - Tectonics of the Simplon massif and Lepontine gneiss dome: deformation structures due to collision between the underthrusting European plate and the Adriatic indenter. Swiss Journal of Geoscience, 101, 515–546.

Thapa B.B., Nolting R.M., Teske M.J, Mcrae M.T. (2005) - Predicted and observed groundwater inflows into two rock tunnels - RECT Proceedings, Chapter 50, p. 556-567.

Thornthwaite C.W., Mather J. R. (1957) - Instructions and tables for computing potential evapotranspiration and the water balance. Drexel Institute of Technology, Publications in Climatology, Vol. X, 3, 185-311 p, Centerton, New Jersey (USA).

Urey H. C., Lowenstam H. A., Epstein S., Mckinney C. R. (1951) - Measurement of paleotemperatures and temperatures of the Upper Cretaceous of England, Denmark and the Southern United States. Geological Society of America Bullettin, 62, pp. 399-416.

Zaadnoordijk W.J. (2009) - Simulating Piecewise-Linear Surface Water and Ground Water Interactions with MODFLOW. Ground Water, 47(5), 723–726.

Zheng C., Bennevy G. D. (1995) - Applied contaminant transport modelling - Van Nostrand Reinhold ITP

Zwingmann H., Mancktelow N. (2004) - Timing of Alpine fault gauges. Earth and Planetary Science Letters, 223, 415-425.



DOI 10.4409/Am-021-10-0017